

2017 年度

修士論文

CORN HEIGHT ESTIMATION USING UAV FOR CROP
MONITORING AND YIELD PREDICTION

UAV を用いた圃場モニタリングのためのトウモロコシの植生高推
定と収穫量子測

FLAVIO FURUKAWA

フルカワ フラビ

オ

201631011

指導教員 酪農学専攻 環境GIS研究室 教授 金子正美

酪農学園大学大学院酪農学研究科

Title: "CORN HEIGHT ESTIMATION USING UAV FOR CROP MONITORING AND YIELD PREDICTION"

Flavio Furukawa

[Introduction]

The world population will reach 9.1 billion people by 2050 and feed this entire population an increase of food production is necessary, moreover, the challenge is to increase food production sustainably, without damaging the natural environment. One of the tools capable to reach this goal is Precision Agriculture, through techniques such as Variable Rate Application (VRA), which enables a decrease in usage of fertilizers and pesticides, followed by a possible increase of crop productivity without area expansion.

Technologies such as Geographic Information System (GIS) and Remote Sensing are fundamental to understand crop conditions, providing different types of information such as crop health, plant growth stages, plantation layout, along with others, being essential to apply Precision Agriculture techniques. Unmanned Aerial Vehicle (UAV) is one of the Remote Sensing platforms, which consists of aircrafts controlled remotely to acquire high spatial and temporal resolution aerial data for different purposes including agriculture.

This study aimed to predict corn crop yield through corn height estimation generated through 3D photogrammetry with UAV imagery based on Structure from Motion technology (SfM), and crop monitoring comparing along with the Normalized Difference Vegetation Index (NDVI), a vegetation index widely used for agricultural purposes.

[Methodology]

The experiment was conducted in a corn field of 363.48 square meters divided into 36 grids at Rakuno Gakuen University, Hokkaido, Japan, seeded with the hybrid 36B08 on May 1st, 2017. Between May and September, fourteen flights campaign were made to acquire RGB, 3D, and NDVI data, using commercial quadcopters.

The acquired data was processed through SfM technology, creating orthomosaics and dense point clouds as output to perform different analyses through GIS and Remote Sensing technologies such as corn height estimation, NDVI analysis, crop growth monitoring. After processing, those data were compared with the dataset obtained in harvest through a ground survey made in middle October.

[Results]

For this specific corn hybrid (36B08), a low correlation between Field Measured Height (FMH) and crop yield was found, spoiling the possibility to estimate crop yield through height, consequently, alike happened using UAV Height Estimation (UHE) over time. Despite, corn height estimation through UAV presented a potential to estimate height for crop monitoring, presenting an expressive correlation with FMH ten weeks before harvest. Comparing with NDVI, UHE could identify crops' growth more clearly in late stages and also monitor growth after NDVI reaches its saturation.

タイトル：「UAV を用いた圃場モニタリングのためのトウモロコシの植生高推定と
収穫量予測」

フルカワ フラビオ

[目的]

世界の人口は 2050 年までに 91 億人に達し、この人口全体に食糧生産を増やす必要がある。また、自然環境を損なうことなく持続的に食糧生産を増やすことが課題である。この目標を達成できるツールの 1 つは精密農業であり、肥料や農薬の使用を減らすことが可能な VRA (Variable Rate Application) などの技術によって、面積拡大なしで作物生産性を高める可能性がある。

地理情報システム (GIS) やリモートセンシングなどの技術は、農作物の健康状態、植物の生育段階、プランテーションのレイアウトなどさまざまな種類の情報を提供して精密農業技術を適用する上で不可欠な作物の状態を把握するための基礎的要素である。無人航空機 (UAV) は、リモートセンシングのプラットフォームの 1 つであり、農業を含むさまざまな目的のために空間および時間的高解像度なデータを取得するために遠隔制御される航空機である。

この研究は、SfM (Structure from Motion technology) に基づき、UAV 画像を用いて 3D 写真測量によりトウモロコシの植生高を推定し作物収量の予測を目的とした。また精密農業分野で広く使用されている指数である NDVI (Normalized Difference Vegetation Index) と作物モニタリングの結果との比較を行った。

[方法論]

実験は、2017年5月1日にハイブリッド36B08を植えた北海道Rakuno Gakuen大学の363.48平方メートルのトウモロコシ畑で行われた。5月から9月の間に計14日間の商用クワッドコプターを使用して撮影を行った。

取得されたデータは、SfM技術によって処理され、オルトモザイクおよびポイントクラウドを出力として生成し、GISおよびリモートセンシング技術によってコーン高さ推定、NDVI分析を行った。処理後、これらのデータは、収穫時に得られたデータセットと、10月中旬に実施された地上調査と比較した。

[結果]

この特定のトウモロコシ雑種(36B08)について、野外測定高さ(FMH)と作物収量との間の低い相関であった。(図2)これはUAV高さ推定(UHE)を使用しても作物収量を推定できる可能性は低いことを示す。一方でUAVを通じたトウモロコシの高さ推定は作物モニタリングのための高さを推定する可能性を示し、収穫の10週間前にFMHとのやや強い相関を示した(図3)。

NDVIと比較して、UHEは後期に作物の成長をより明確に識別し、NDVIが飽和に達した後の成長を監視することができた。

CONTENTS

1. Introduction	1
2. Materials and Methods.....	5
2.1. Materials	5
2.1.1. Unmanned Aerial Vehicle	5
2.1.2. Photogrammetry	6
2.1.3. Commercial UAV.....	7
2.1.4. Flight Path Design Application.....	8
2.1.5. NDVI Reflectance Calibration.....	10
2.1.6. Photogrammetry Software.....	12
2.1.7. 3D Data Edition	14
2.1.8. Remote Sensing and GIS Software.....	15
2.2. Site Description and Management.....	16
2.3. Data Acquisition.....	18
2.4. Data Processing	22
2.4.1. NDVI.....	23
2.4.2. Height Estimation	26
3. Results.....	27

3.1 NDVI Assessment.....	27
3.2 UAV Height Estimation Assessment.....	31
3.3 NDVI and UAV Height Estimation through time.....	32
3.4 Field Data	36
3.5 Correlations through Time	40
3.6 Crop Monitoring	44
4. Discussion.....	46
5. Conclusions	51
6. Acknowledgments.....	52
7. References.....	53

LIST OF TABLES

Table 1: Number of images taken for each dataset	19
Table 2: Data measured on the field on October 14th	37

LIST OF FIGURES

Figure 1: Phantom 4 Pro, Phantom 3 Professional and NDVI lens from Peau Productions Inc.	7
Figure 2: Pix4D Capture app - Path design for 3D Model data acquirement .	8
Figure 3: Map Pilot app - Path design for IR+R and RGB data acquirement .	9
Figure 4: Mapir Camera Reflectance Calibration Ground Target	10
Figure 5: Example of IR+R data before and after calibration	11
Figure 6: Photogrammetry workflow	12
Figure 7: Agisoft Photoscan Professional, image alignment and 3D model.	13
Figure 8: Cloud Compare V2.8.1 Stereo	14
Figure 9: Study area in south-west side of Rakuno Gakuen University, Hokkaido	16
Figure 10: Field grids and respective sizes expressed in meters.....	17
Figure 11: Data acquirement dates, between May and September 2017	18
Figure 12: Mapir Camera Reflectance Calibration Ground Target taken with Phantom 3 Professional + NDVI lens.....	20
Figure 13: NDVI roof reference for time series data normalization	24
Figure 14: Digital Globe's World View 2 Imagery from July 13th with 50 centimeters resolution.....	25
Figure 15: NDVI Correlation between UAV Imagery and WV2 Imagery on July 13th	28
Figure 16: NDVI Correlation between UAV Imagery from August 17th and WV2 Imagery from August 23rd.....	28
Figure 17: NDVI Correlation between UAV Imagery from September 7th and GE1 Imagery from September 1st	29

Figure 18: Normal NDVI vs Green Coverage NDVI through time	30
Figure 19: Correlation between Green Coverage NDVI and Normal NDVI ..	30
Figure 20: Correlation between UAV Height Estimation from September 7th and Field Measured Height from October 14 th	31
Figure 21: NDVI average and UAV Height Estimation average through time	32
Figure 22: NDVI average and UAV Height Estimation average between May 26th and June 27th	33
Figure 23: NDVI average and UAV Height Estimation average between June 27th and August 17th.....	34
Figure 24: NDVI average and UAV Height Estimation between August 2nd and September 7th	35
Figure 25: Correlation between Dry Matter measured in the field and Field Measured Height.....	38
Figure 26: Correlation between Dry Grain Yield and Field Measured Height	39
Figure 27: Correlation between UAV Height Estimation and Dry Matter through time	40
Figure 28: Correlation Between UAV Height Estimation and Dry Grain Yield through time	41
Figure 29: Correlation between NDVI and Dry Matter through time	42
Figure 30: Correlation between NDVI and Dry Grain Yield through time	42
Figure 31: Correlation between Field Measured Height and UAV Height Estimation through time	43
Figure 32: UAV Height Estimation throughout time.....	44
Figure 33: NDVI from UAV throughout time	45
Figure 34: Different soil moisture among June 16th, 20th, and 27th.....	47
Figure 35: Dense point cloud of June 7th	48

1. Introduction

By 2050, the world's population will reach 9.1 billion, an increase of 34 percent comparing to 2009, mostly in developing countries, with 70 percent of the population living in urban areas (FAO, 2009) . To feed this entire population, an increase of 70 percent in food production is necessary. As an example, the annual cereal production has to reach 3 billion tons by 2050, in 2009 the annual cereal production was 2.1 billion tons.

Despite that fact, another challenge is to feed this population sustainably, increase food production considering the safety and conservation of the natural resources. The sustainability concept is based on the principle that the needs of the present are met without compromising the needs of the future (Spiertz, 2009). Pretty (2008) introduced that the sustainability demands a development in agricultural technologies and practices that do not affect the environment, leading a growth in food quality and production with minimum side effects against the environment.

One of the technologies mentioned by Pretty (2008) is called Precision Agriculture. A generic definition for this term, quoted by McBratney et al. (2005) says: "that kind of agriculture that increases the number of (correct) decisions per unit area of land per unit time with associated net benefits", in other words, an increase of quality and/or quantity of production, reducing environmental hazards derived from excessive inputs (fertilizers and pesticides) application, increasing their usage efficiency and even reducing them, through variable management practices (Tang and Turner, 1999). As R. Bongiovanni and Lowenberg-Deboer (2004) instanced, the concepts between sustainability and

precision agriculture are linked, using agricultural machinery coupled with Global Navigation Satellite System (GNSS), the application of fertilizers and pesticides where and when they are needed became possible. Called as Variable Rate Application technique - a concept published by The University of Illinois back in 1929 (Sawyer, 2013) – the usage of fertilizers and pesticides more accurately on the crops generates more possibilities to reduce their usage, reaching only the interested area, improving plant health, reducing costs, and collaborating to reduce environmental damages.

Geographic Information Systems (GIS) and also with the improvements in spatial and temporal resolutions of Remote Sensing technologies in different platforms (satellites and aircrafts), strengthen the suitability for Precision Agriculture technique (Matese et al., 2015). Capable to acquire fairly reliable field data through a nondestructive method, delivering measurement data through the electromagnetic spectrum, allowing the assessment and monitoring of the crop chlorophyll status, spatial distribution of the crop, addressing important issues such as crop growth monitoring, vegetation stress detections, different predictions and improvement of crop management practices (Haboudane et al., 2008).

Unmanned Aerial Vehicles (UAVs) is a platform inside the Remote sensing technology which has been highlighted due the low cost and high spatial/ temporal resolutions that it offers (Salamí et al., 2014). UAVs, also known as drones, are being widely used for Precision Agriculture purposes, capturing imagery for plant/ crop analysis, acquiring information on soil water holding and irrigation systems (Ipate et al., 2015). This technology is based in an aircraft controlled remotely by a human or computer, coupled with a digital camera and/or different types of sensors (multispectral, LIDAR, thermal, etc.)

to acquire data of a specific scenario. Using photogrammetric techniques, those acquired data can result in image orthomosaics and point dense clouds (Rokhmana, 2015).

Vegetation indexes is one of the products derived of UAVs coupled with multispectral sensor. Normalized Difference Vegetation Index, also known as NDVI, developed by Rouse et al. (1973) is a widespread vegetation index in the Precision Agriculture and natural environment fields. An index calculated from the normalized total reflectance from infrared and red bands, it is used to estimate vegetation health condition and vegetation changes through the time. The study made by Huang et al. (2014) also found a strong correlation between NDVI data and crop yield, being possible to establish crop yield estimation models, even without any historical crop yield records.

Another result obtainable through UAV platform is the 3D point cloud, an output that can be obtainable through laser systems (LIDAR) or 3D photogrammetry technology. Structure from Motion (SfM) technique is a low cost photogrammetry technology that recreates a structure by overlapping a set of offset images, using the principles of stereoscopic photogrammetry (Westoby et al., 2012). The stereoscopic technique creates the illusion of depth, simulating the human binocular vision (Ortiz et al., 2013), which sees the same scenario with a slight different angle from each eye, generating a 3D point cloud. Each point has its own position information (X, Y, and Z) representing different structures' dimension in a 3D environment, enabling different analysis of the 3D model.

The present research aims to estimate the height of a corn crop field, using a non-modified commercial UAV (DJI Phantom 4 Pro), through 3D photogrammetry technology for corn crop yield estimation and growth

monitoring since Yin et al. (2011) affirms that early to mid-season crop plant height is reliable as a predictor of corn yield, which also has a strong relationship with nitrogen (N) application rate, confirming with Raun et al. (2001), which refers that grain yield goals is the most reliable method to estimate pre plant fertilizer N rates. Along with that, understand the plant height growing rate comparing with the widely used vegetation index on the Precision Agriculture field, the NDVI.

2. Materials and Methods

2.1. Materials

2.1.1. Unmanned Aerial Vehicle

UAV terminology stands for Unmanned Aerial Vehicle, in other words, an aircraft without a pilot on board, controlled remotely by human or a computer. UAVs are extensively used for different industries such as film productions, disasters management, rescue operations, military purposes, law enforcement and border control surveillance, aerial photography for journalism, and also for agricultural and environmental purposes.

In order to acquire data through UAV, a mounted sensor is necessary. It is possible to mount sensors such as RGB camera, multispectral sensor, thermal sensor, laser scanner (LIDAR), etc. For most regular photogrammetric purposes, an ordinary RGB camera is capable to generate image orthomosaics, point dense clouds, and digital elevation models through photogrammetry methods.

2.1.2. Photogrammetry

Photogrammetry is the science to extract from images, the form, dimensions, and position of the objects and/or surfaces contained therein. Applying a technique called Structure from Motion (SfM), which consists in advanced algorithms to recreate 3D structures from overlapped 2D imagery, outputs such as image orthomosaics, point dense clouds, and DEM (Digital Elevation Models) are created. This technique is based stereovision principle, which compares the same scene from different angles to match common points, it works as the human eyes, which can detect the perception of depth, looking to the same scene with a slight different angle from each eye.

2.1.3. Commercial UAV

In this research two quadcopter type UAVs were used, the DJI Phantom 3 professional, coupled with a 3.97mm NDVI lens from Peau Productions Inc. (Figure 1), a special lens with no filter, allowing all wavelengths of light reach the sensor, separated into infrared and red bands on the Blue and Red channel respectively; and the DJI Phantom 4 Pro with no modification along with an iOS tablet with Pix4D Capture and Map Pilot application to design flight path and control the flight for both UAVs remotely.

DJI is a Chinese company based in Shenzhen, China, which produces different types of UAVs for different industries. The Phantom series is the DJI consumer flagship quadcopters, it is being used for different industries which goes from film production to agricultural monitoring.

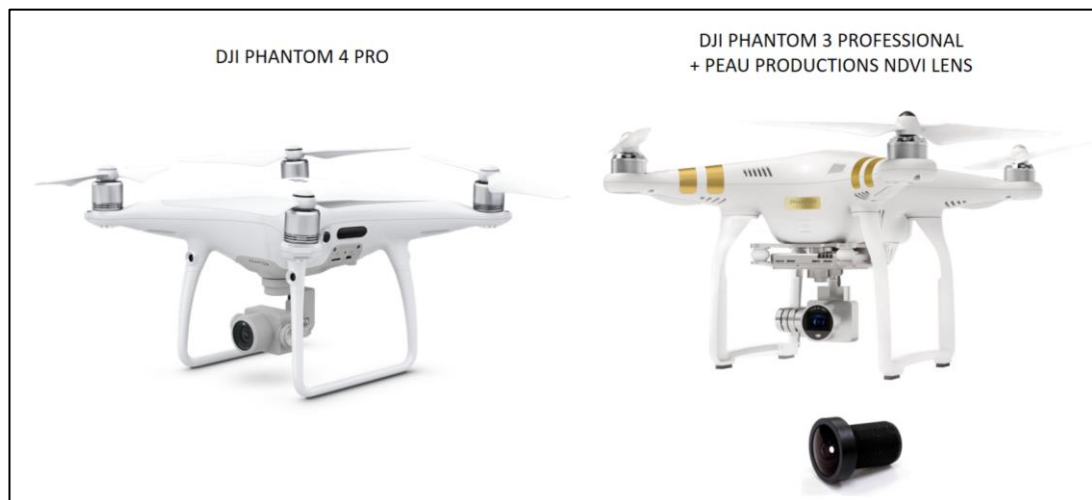


Figure 1: Phantom 4 Pro, Phantom 3 Professional and NDVI lens from Peau Productions Inc.

2.1.4. Flight Path Design Application

Pix4D Capture (Figure 2) is a ground station application for iOS and Android devices which enables the ability to design a specific path for 3D models, exporting all images in JPEG format. It is possible to set the angle of the camera at 70 degrees, enabling the visualization of the sides of the structure, to create more accurate 3D models. Another ground station used in this research was the Map Pilot (Figure 3), from Maps Made Easy, differently from Pix4D Capture, this application has the capability to shoot raw images (DNG format), which is essential to perform reflectance calibration on the acquired infrared and red bands data from NDVI lens

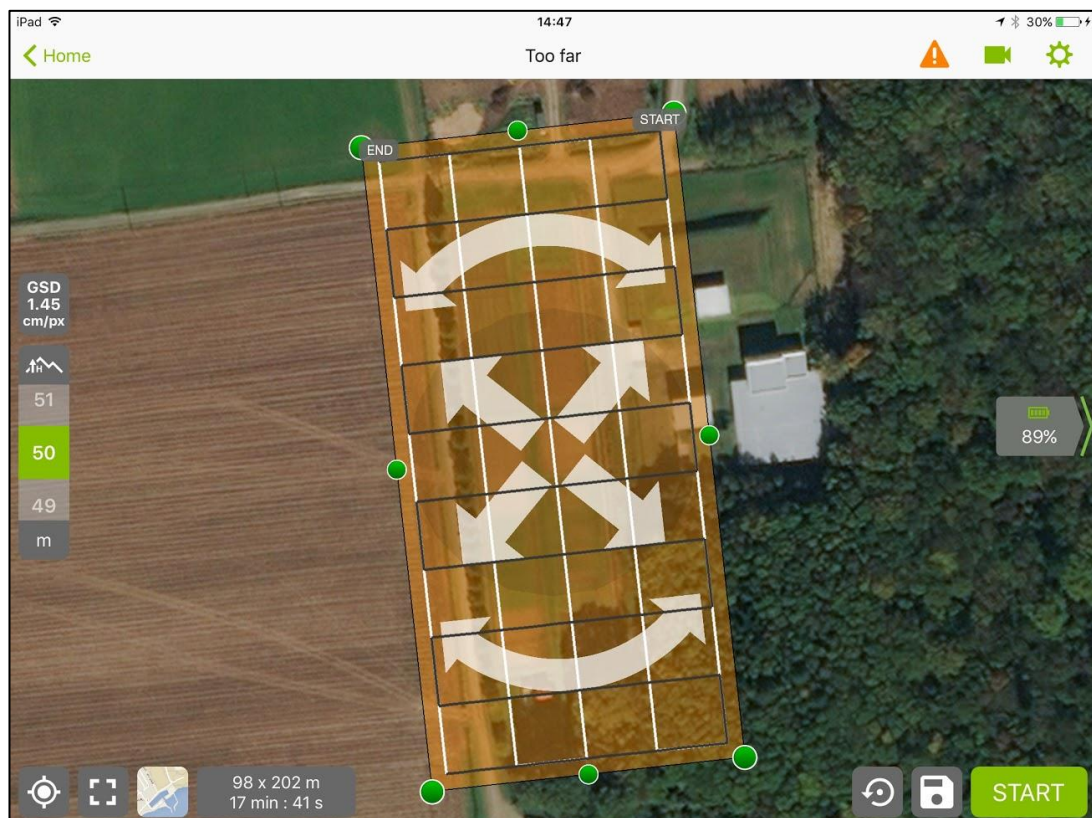


Figure 2: Pix4D Capture app - Path design for 3D Model data acquisition

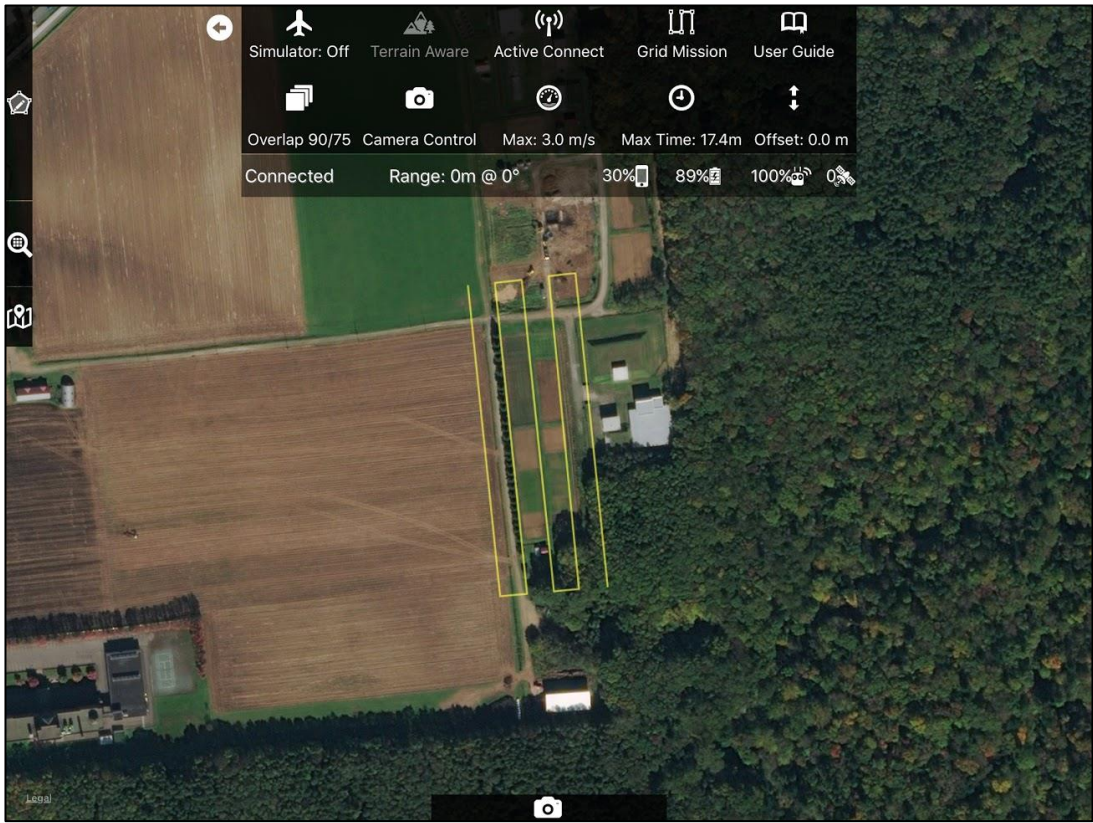


Figure 3: Map Pilot app - Path design for IR+R and RGB data acquirement

2.1.5. NDVI Reflectance Calibration

For the calibration of the infrared + red images from DJI Phantom 3 Professional plus the NDVI lens, the Mapir Camera Reflectance Calibration Ground Target (Figure 4) is required, using the QGIS plugin named Mapir Processing Plugin, the values obtained through the modified UAV is transformed into reflectance values (Figure 5), which results in more accurate NDVI datasets.



Figure 4: Mapir Camera Reflectance Calibration Ground Target



Figure 5: Example of IR+R data before and after calibration

2.1.6. Photogrammetry Software

To apply the SfM technique, Agisoft Photoscan Professional (Figure 7) is a software that creates image orthomosaics and 3D models, the process consists in basically three steps: photo-alignment, point cloud and mesh, and outputs (**Error! Reference source not found.**).

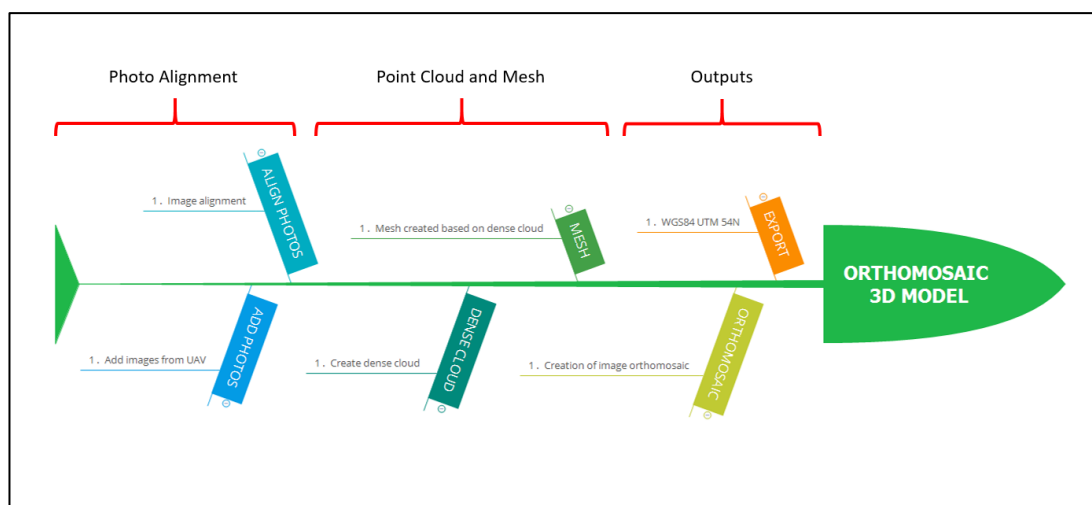


Figure 6: Photogrammetry workflow

The first process is to add the images from the UAV into the software (in case of NDVI data it has to be converted first to tiff format), following that, the key points of the overlapped 2D images are extracted for image matching. The accuracy of alignment influences the output, which is possible to preset in the software, but higher accuracy requires more time for computation. The second step is the creation of dense cloud and mesh, the algorithm inside the software calculates depth information and builds the dense point cloud and mesh. In the final process, the software creates files that can be exported into digital surface models, orthomosaics, and 3D models. The simulation of a

LIDAR file format (.las) is also exportable using the dense point cloud, enabling data edition in LIDAR software, such as Cloud Compare Stereo.

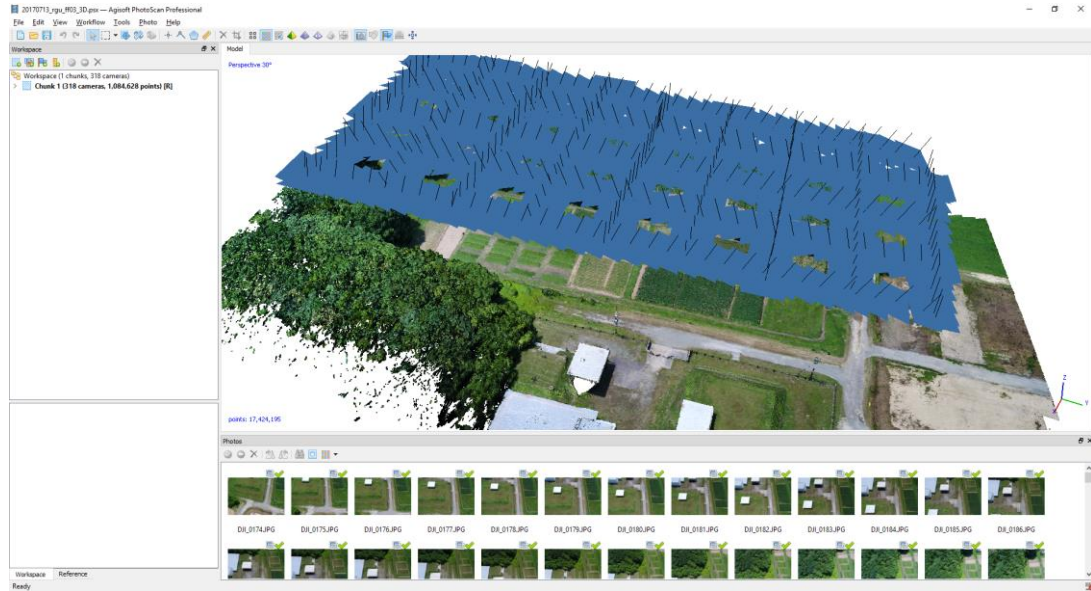


Figure 7: Agisoft Photoscan Professional, image alignment and 3D model

2.1.7. 3D Data Edition

The dense point cloud created with Agisoft Photoscan Professional can be edit in Cloud Compare V2.8.1 Stereo (Figure 8), an open source software which allows a very fine dense point alignment through a function called Cloud Registration, which has an algorithm to register two entities called Interactive Closest Point, minimizing the difference between two dense point clouds, in this study the ground was used as reference for alignment.

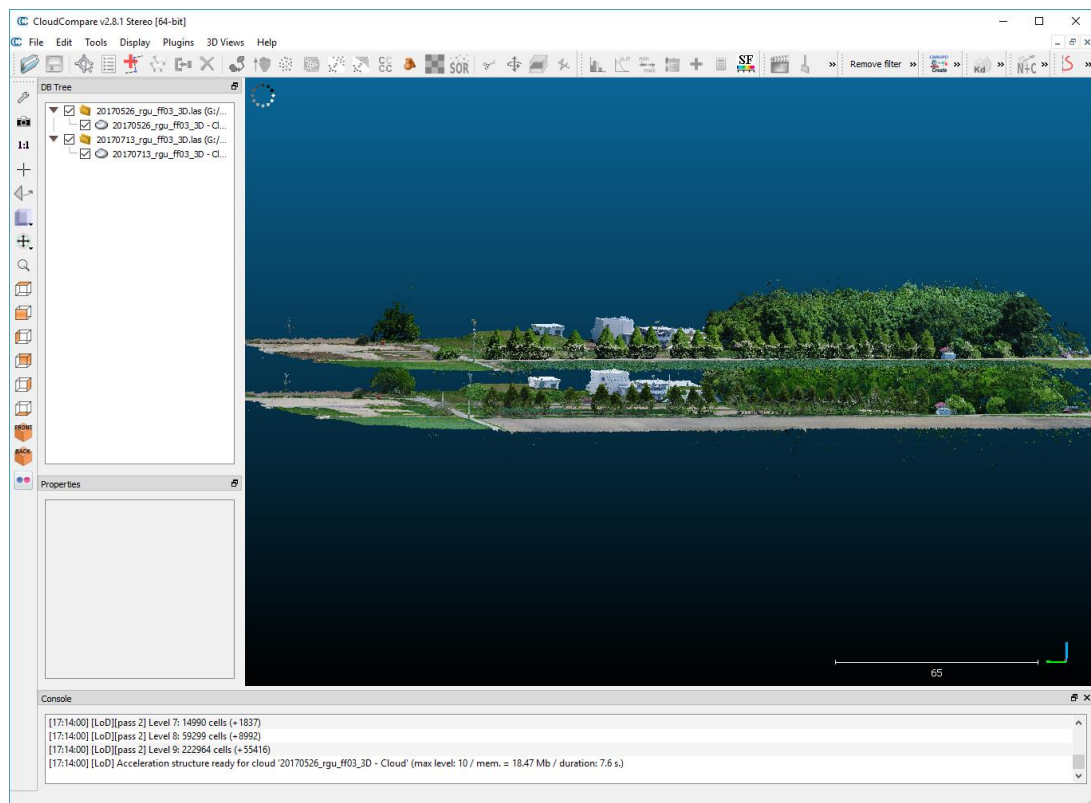


Figure 8: Cloud Compare V2.8.1 Stereo

2.1.8. Remote Sensing and GIS Software

Remote Sensing and GIS software are essential to compare UAV datasets. Envi 5.4 is a Remote Sensing software that have the capability to manage multispectral data and perform different analysis, whereas Esri's ArcMap 10.5 with the Spatial Analyst toolbox has the tools to perform spatial data processing, including functions to convert data, georeference data, calculate indexes, extract geospatial information from multispectral data through shapefiles, etc. Along with that, through those software is possible to compare datasets from different Remote Sensing platforms such as satellite imagery and UAV imagery.

2.2. Site Description and Management

The experiment was conducted on a field located at south-west of Rakuno Gakuen University (Figure 9), Hokkaido, Japan. A field of 363.48 square meters was divided into 36 grids, created with wood stacks and strings, containing 6 rows and 6 columns, named from E1 to E36 (Figure 10). In the first 5 rows, each grid had 3.8m x 2.6m and the last row each grid had 4.3m x 2.6m. The shapefile of the grid was transcript through ArcMap 10.5 with the RGB georeferenced UAV data from May 26th as a reference.

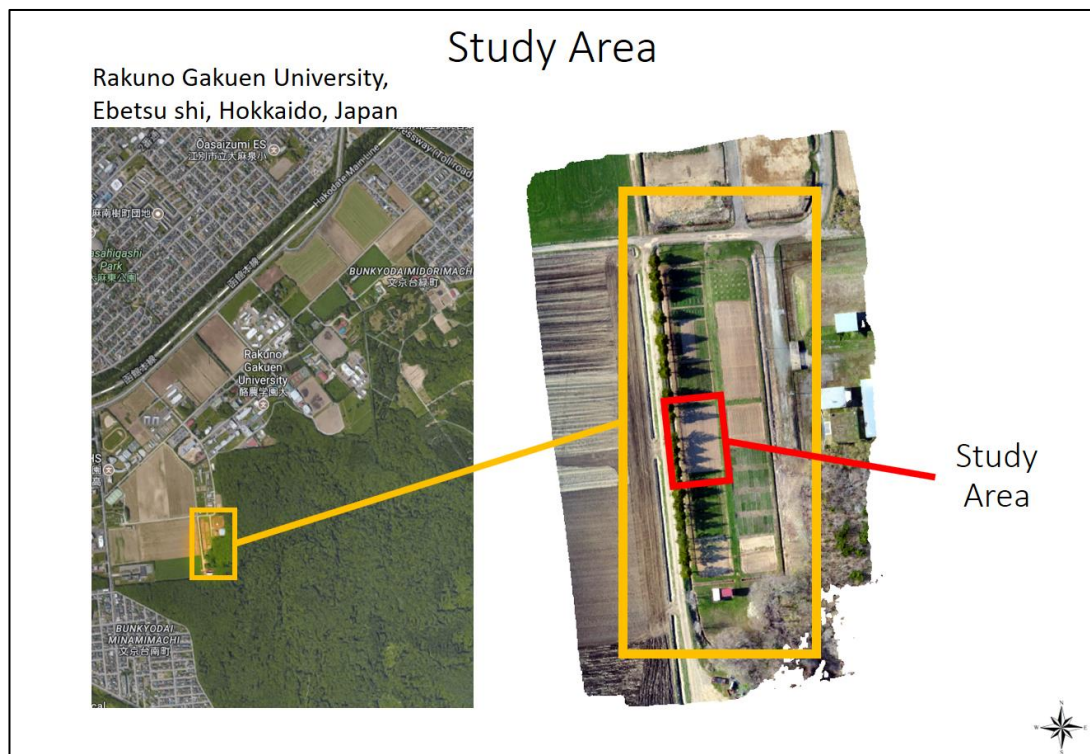


Figure 9: Study area in south-west side of Rakuno Gakuen University, Hokkaido

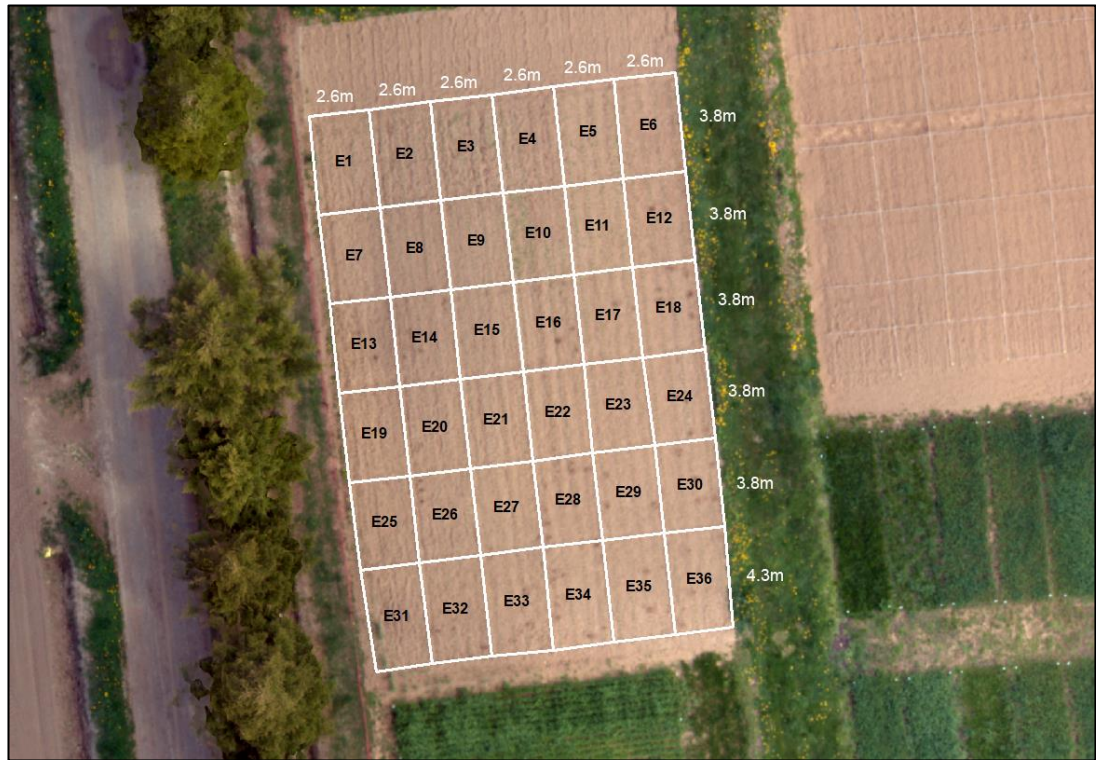


Figure 10: Field grids and respective sizes expressed in meters

The seeding of hybrid corn 36B08 from Pioneer Hi-Bred International, was made on May 1st, 2017 using a manual seeder, with each grid receiving a different treatment during the season. Harvest was made on October 14th of 2017. For data comparison, 10 samples of each grid were collected on harvest day, obtaining the average of plant height of each grid in centimeters, total dry matter in g/m^2 and dry grain yield in g/m^2 .

2.3. Data Acquisition

For data acquisition, two UAVs were used, a DJI Phantom 3 Professional with NDVI 3.97mm lens from Peau Productions Inc. and an out-of-the-box DJI Phantom 4 Pro. From May to September, three flights were performed almost every week, acquiring NDVI, RGB, and 3D data, totaling 42 flights in 14 weeks (Figure 11 and Table 1)

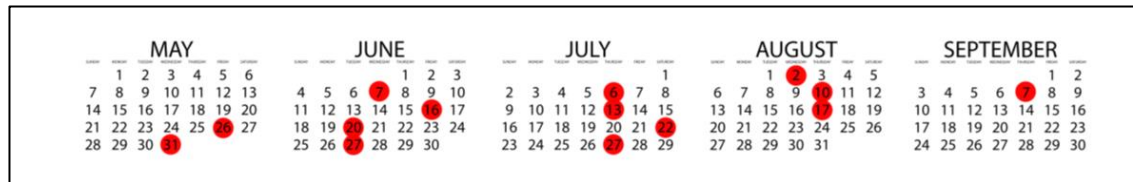


Figure 11: Data acquisition dates, between May and September 2017

Number of images			
Date	3D (Pix4D)	RGB (Map Pilot)	IR+R (Map Pilot)
26-May	314	109	267
31-May	313	108	204
7-Jun	318	110	204
16-Jun	319	173	212
20-Jun	314	169	213
27-Jun	315	170	213
6-Jul	319	171	211
13-Jul	318	173	213
22-Jul	317	169	212
27-Jul	319	168	211
2-Aug	317	166	198
10-Aug	316	175	220
17-Aug	319	197	214
7-Sep	316	180	210

Table 1: Number of images taken for each dataset

NDVI data was acquired using the Phantom 3 Professional with a Peau Production Inc. NDVI lens and Map Pilot application on an iOS tablet, flying at 50 meters above the ground, angle of the camera at 90 degrees, setting an overlap of 90 percent and side-lap of 70 percent, with white balance set at auto mode, ISO 100, shutter speed of 1/1000 and DNG file format. After flying over the study field, a shot of Mapir Camera Reflectance Calibration Ground Target

was taken to be used as a reference for reflectance values conversion (Figure 12).

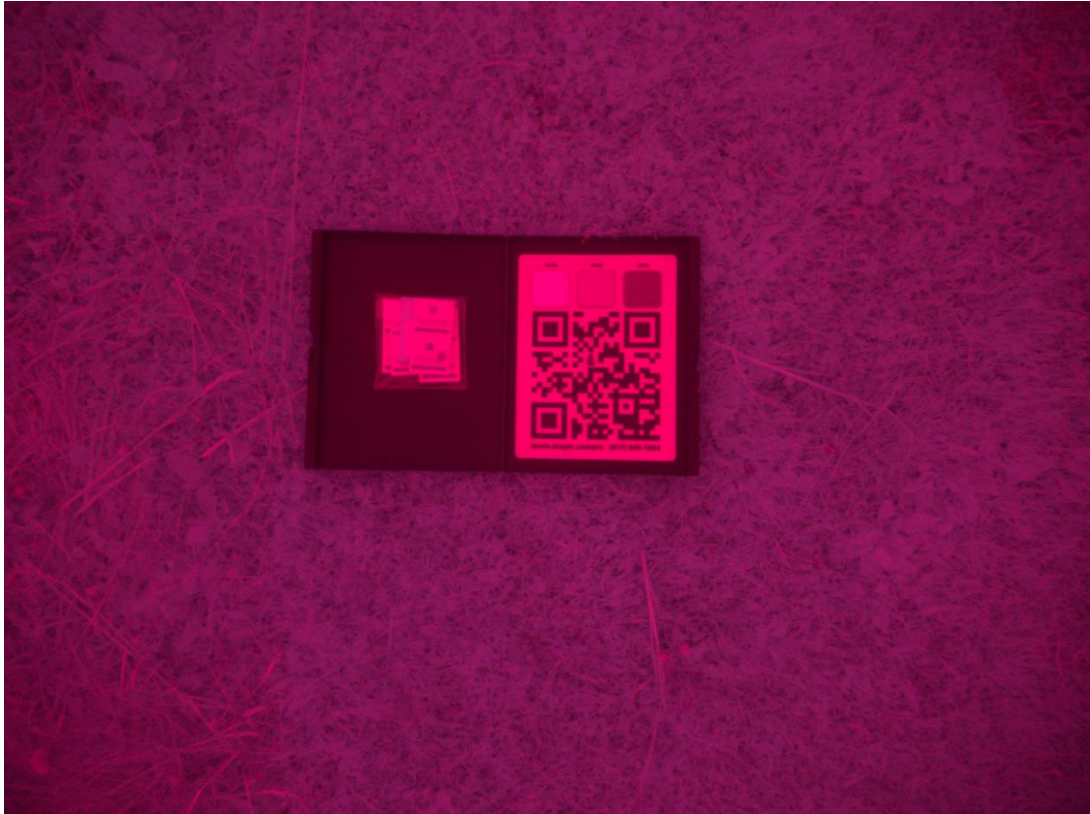


Figure 12: Mapir Camera Reflectance Calibration Ground Target taken with Phantom 3 Professional + NDVI lens

RGB data was taken using a DJI Phantom 4 Pro and Map Pilot application for iOS, flying at 50 meters above the ground, using camera settings at auto mode, with an overlap of 90 percent and a side-lap of 70 percent, angle of the camera at 90 degrees and DNG file format.

For 3D data, the same DJI Phantom 4 Pro was used with Pix4D Capture application, flying at 50 meters above the ground, angle of the camera at 70

degrees, setting the overlap at 90 percent and side-lap at 70 percent, JPG file format, using the camera at automatic settings, with trigger mode set at fast mode.

2.4. Data Processing

All orthomosaics and point dense cloud were created using Agisoft Photoscan Professional on a Hewlett Packard Z620 workstation running Windows 10 Pro, using medium settings for all processes, align photos, create dense cloud and mesh, applying the projection of WGS84/ UTM zone 54N for every output data. The orthomosaics generated from Agisoft Photoscan Professional had a resolution of approximately 1.5 centimeters. All data were georeferenced in ArcMap 10.5 using a Digital Globe 50 centimeters World View 2 (WV2) Imagery from June 13th of 2017 as a reference.

2.4.1. NDVI

For NDVI processing, after collecting the images obtained with Phantom 3 Professional and the NDVI lens from Peau Productions Inc., all data was converted from DNG file to TIFF file through Mapir Processing Plugin for QGIS and processed on the photogrammetry software. The orthomosaics created through Agisoft Photoscan Professional were calibrated to reflectance values using the Mapir Camera Reflectance Calibration Ground Target image on the same QGIS plugin.

Since the white balance was affected by the weather condition of each day (white balance) the data was taken, a simple normalization, using the roof of a building as reference (Figure 13) were performed using Map Algebra tool on ArcMap. That normalization was made to compare the NDVI behavior through the weeks for each grid

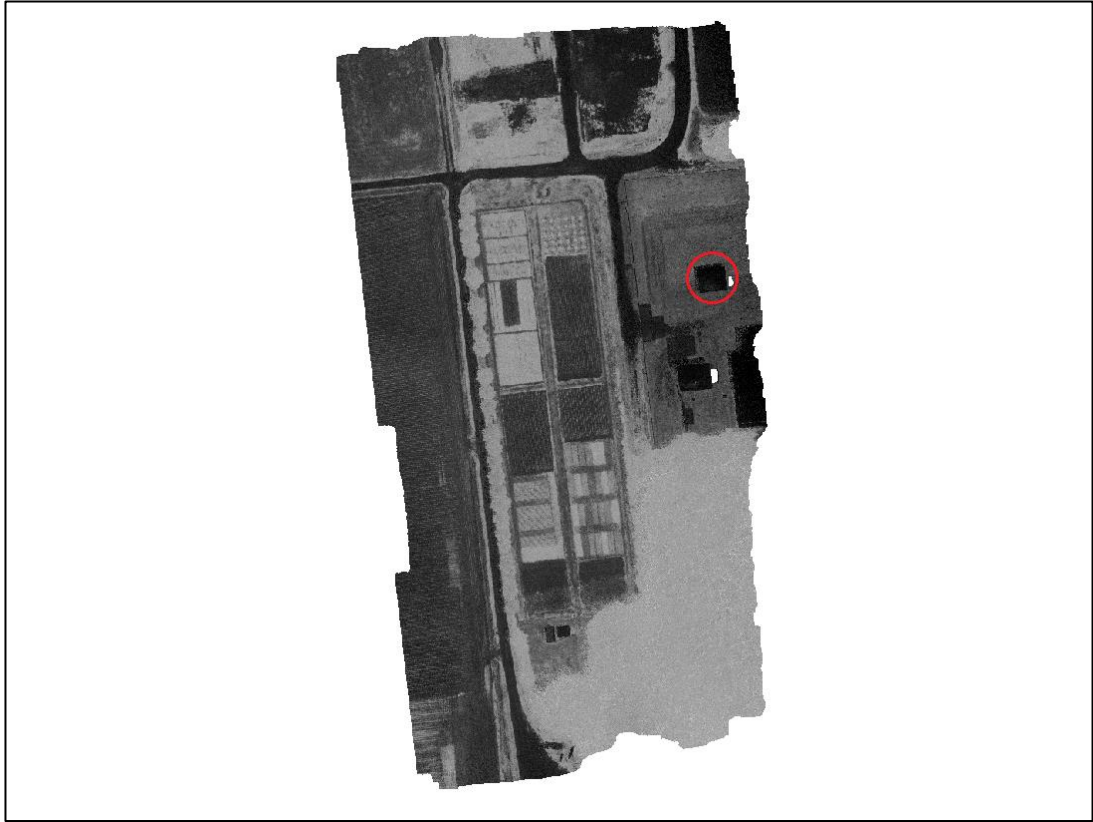


Figure 13: NDVI roof reference for time series data normalization

To assess the accuracy of the NDVI lens from Peau Production Inc., comparisons between the UAV data and radiometric corrected satellite high spatial and spectral resolution imagery (50cm) from Digital Globe, World View 2 (WV2) (Figure 14) and GeoEye 1 (GE1), data were made considering the average of each grid in three periods: July 13th (UAV and WV2), August 17th (UAV) and August 23rd (WV2), and the last one was on September 7th (UAV) and September 1st (GE1). All data was preprocessed in ENVI 5.4, converting DN values in radiometric values. Only in August 23rd, a thin haze was detected affecting on the comparison with UAV data from August 17th.



Figure 14: Digital Globe's World View 2 Imagery from July 13th with 50 centimeters resolution

Green Coverage classification was also performed to extract NDVI values only from the vegetation to understand the influence of different variables such as soil and shade on the NDVI values. Using ArcGIS Interactive Supervised classification tool, every data was classified in two classes, soil and vegetation, a shapefile was created to extract NDVI average for the vegetation of each grid using the Zonal Statistics as Table tool.

2.4.2. Height Estimation

The point cloud generated by Agisoft Photoscan Professional through 3D photogrammetry technique mentioned before, were aligned with Cloud Compare V2.8.1 Stereo software, through Cloud Registration function with May 26th data as a reference for all dataset alignments, setting the final overlap in 30 percent and the random sampling point to 100000.

In ArcMap 10.5, one las dataset was created for each dense point cloud, exported into a raster file for comparison, the georeferencing was also made using WV2 Imagery from July 13th to spatially align all rasters . The Spatial Analyst extension tool was required to calculate height from each week using the Map Algebra tool, with a simple subtraction having May 26th as a ground reference, since there were no plants, the UAV Height Estimation (UHE) were calculated for every week.

3. Results

3.1 NDVI Assessment

The comparison between NDVI lens from Peau Productions Inc. with high spatial/ spectral resolution WV2 and GE1 Imagery, resulted in a significant correlation with both satellites imagery. Considering the average of each grid, on July 13th, the NDVI data from the UAV and the Satellite (WV2) showed an R-Squared of 0.76 (Figure 15). Comparing the data obtained with UAV on August 17th and the data from the WV2 Imagery taken on August 23rd, an R-Squared of 0.527 was found (Figure 16), and this relatively low value on the WV2 Imagery was due the thin haze mentioned before. The last data acquired through UAV was on September 7th and compared to GE1 Imagery from September 1st, an R-Squared of 0.659 was presented (Figure 17).

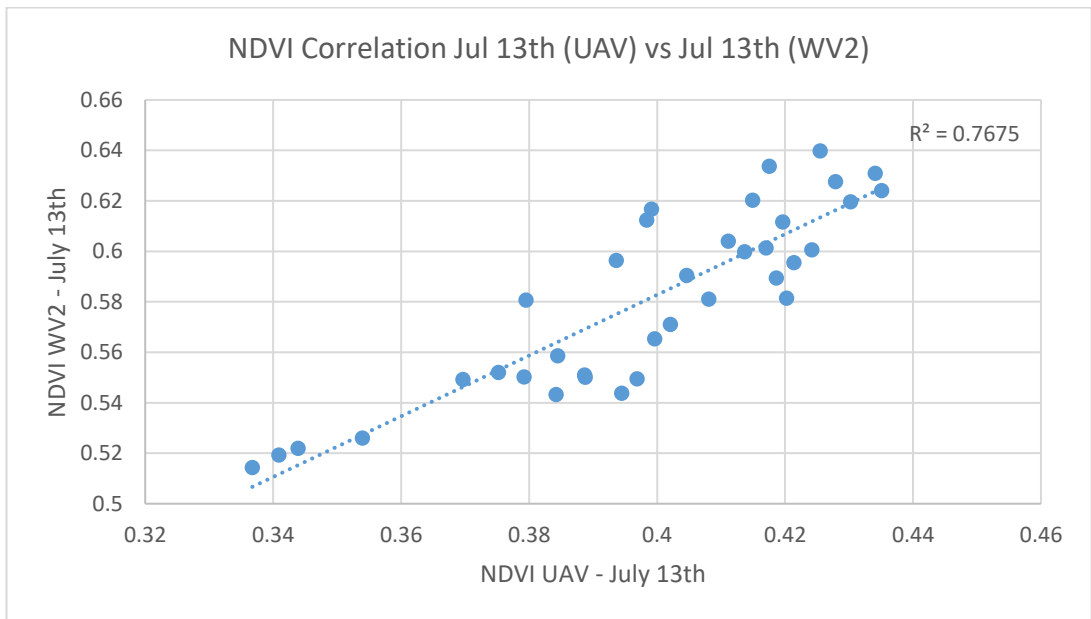


Figure 15: NDVI Correlation between UAV Imagery and WV2 Imagery on July 13th

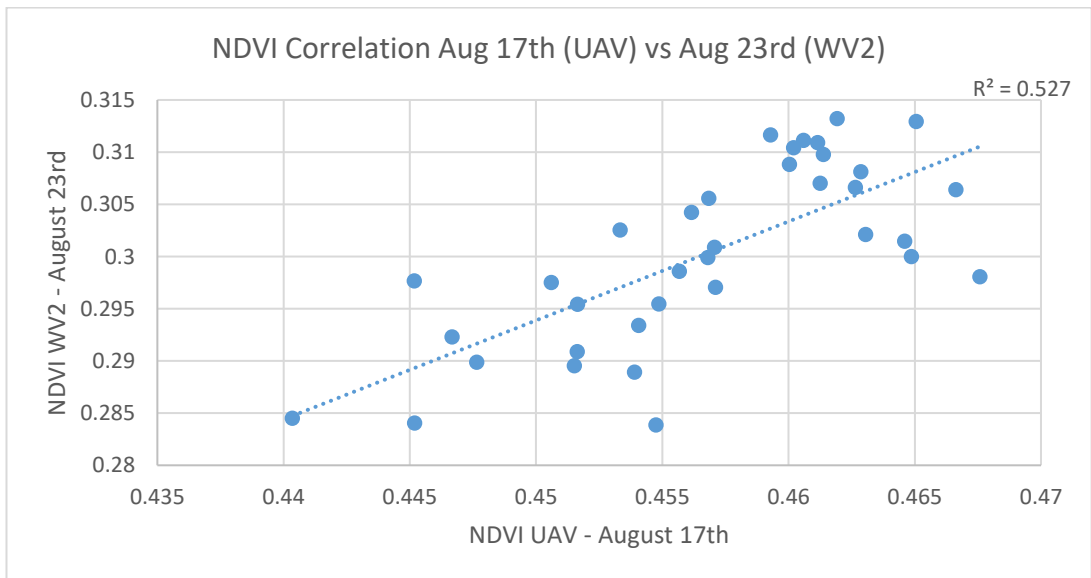


Figure 16: NDVI Correlation between UAV Imagery from August 17th and WV2 Imagery from August 23rd

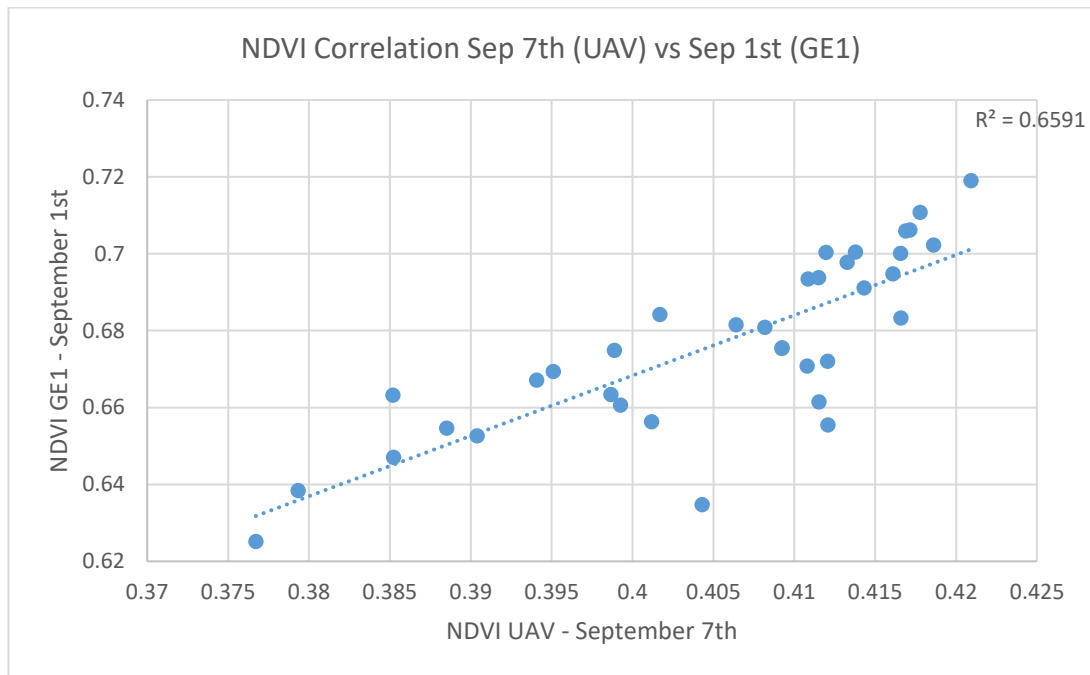


Figure 17: NDVI Correlation between UAV Imagery from September 7th and GE1 Imagery from September 1st

The Green Coverage classification assessment, which was made was to detect the interference of the soil on NDVI values, showed the same pattern of NDVI average without extracting the vegetation through classification (Figure 18), having a correlation of 0.98 between them (Figure 19).

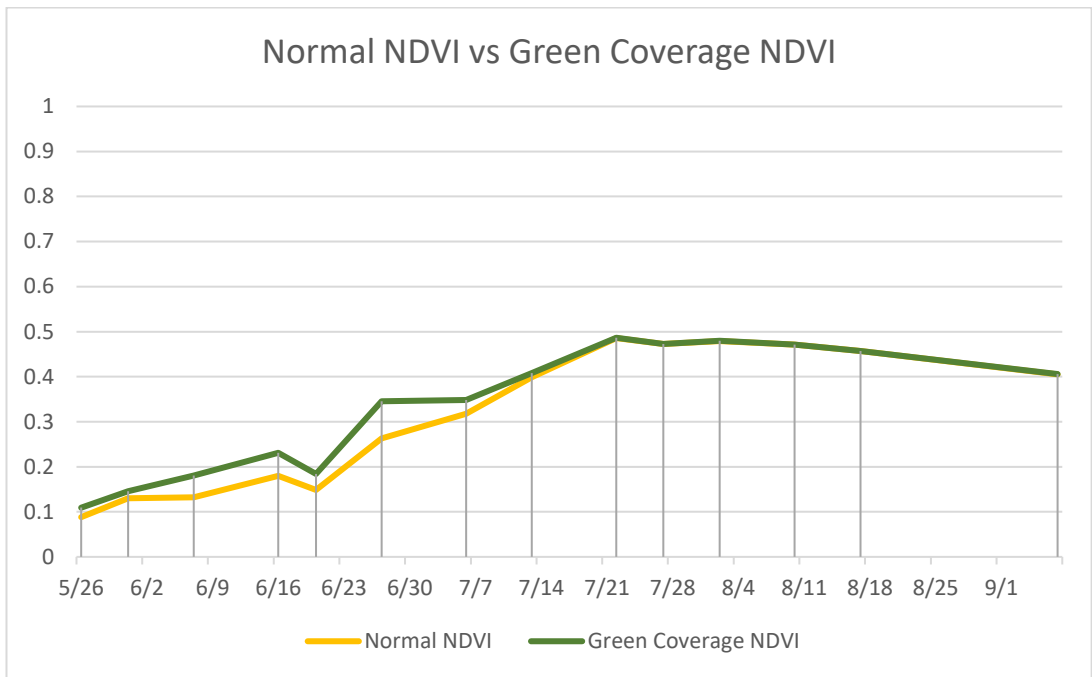


Figure 18: Normal NDVI vs Green Coverage NDVI through time

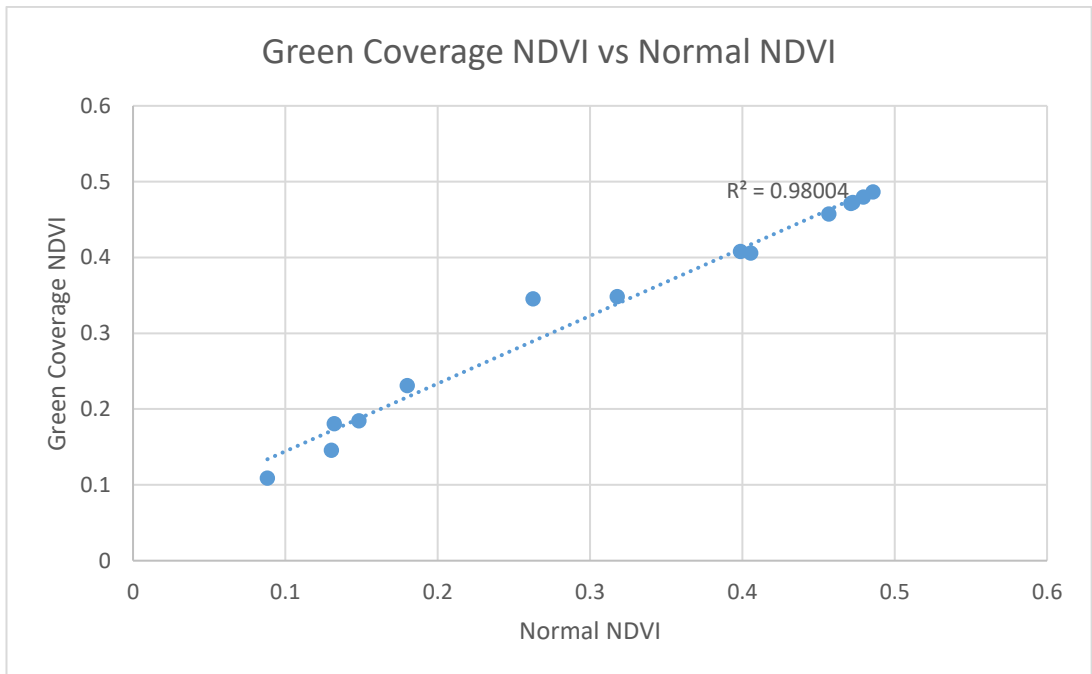


Figure 19: Correlation between Green Coverage NDVI and Normal NDVI

3.2 UAV Height Estimation Assessment

Considering the saturation on UHE field average from August 17th until September 7th, the correlation of each grid average obtained between the UHE and the ground measured height in October 14th was 0.87 (R-Squared) (Figure 20).

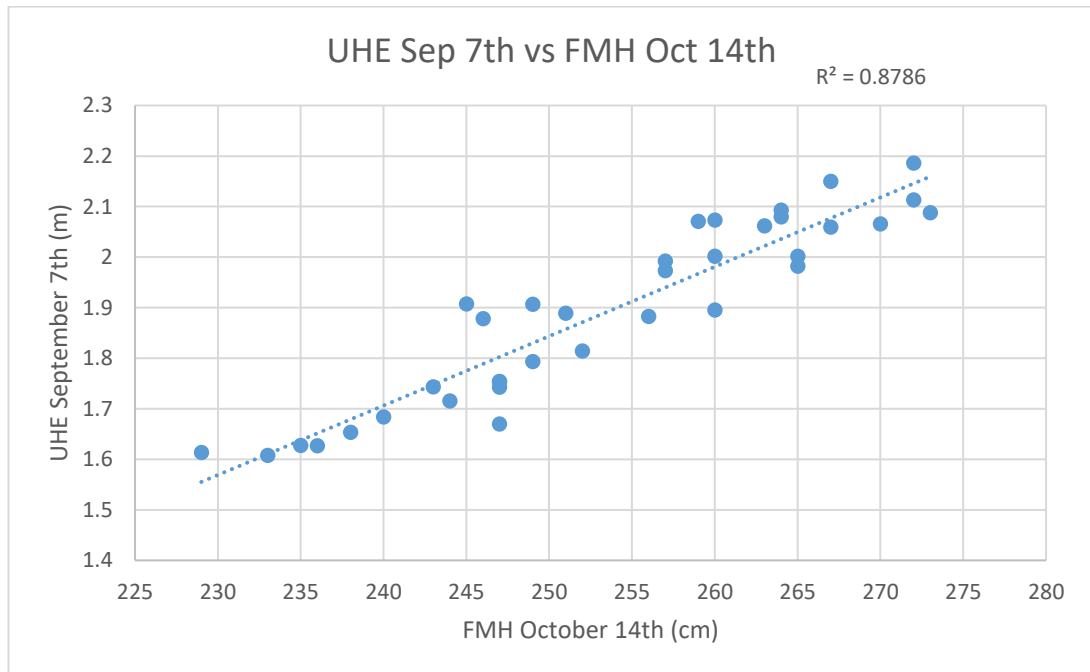


Figure 20: Correlation between UAV Height Estimation from September 7th and Field Measured Height from October 14th

3.3 NDVI and UAV Height Estimation through time

NDVI and UAV Height Estimation (UHE) field averages presented the following characteristics through time (Figure 21):

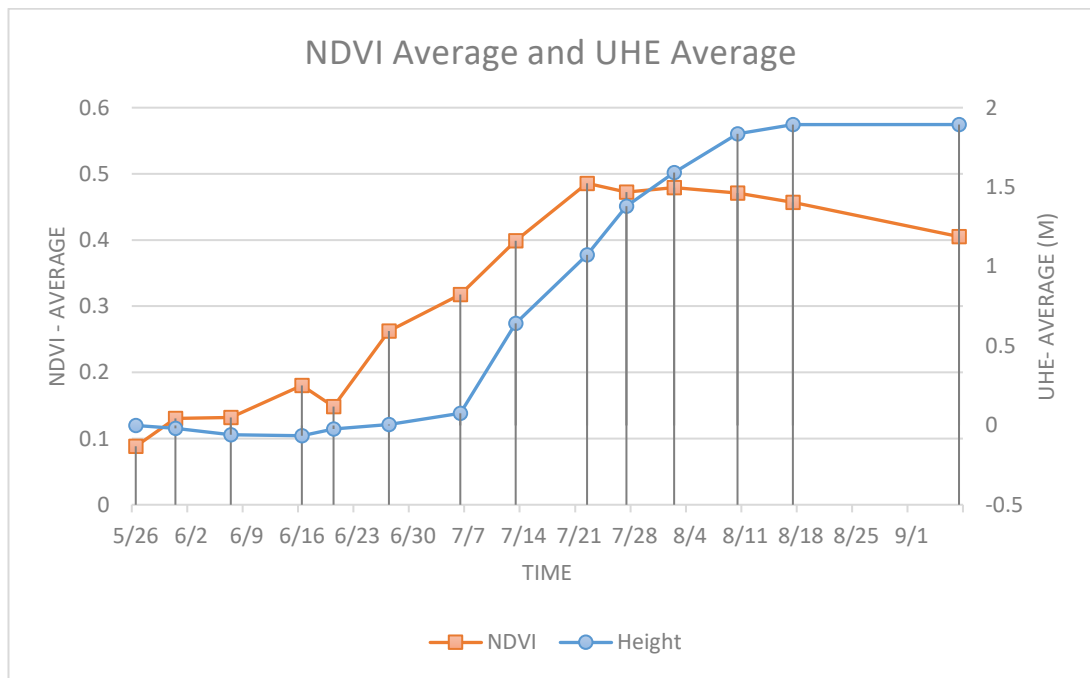


Figure 21: NDVI average and UAV Height Estimation average through time

From May 26th to June 20th, the UHE field average of each grid presented negative values, reaching the lowest value at June 16th – around minus 7 centimeters (Figure 22). On June 27th the UHE field average had the first positive value. On the other hand, NDVI field average showed a constant increase from May 26th until July 22nd, only on June 20th a lower value was found contradicting the increase pattern.

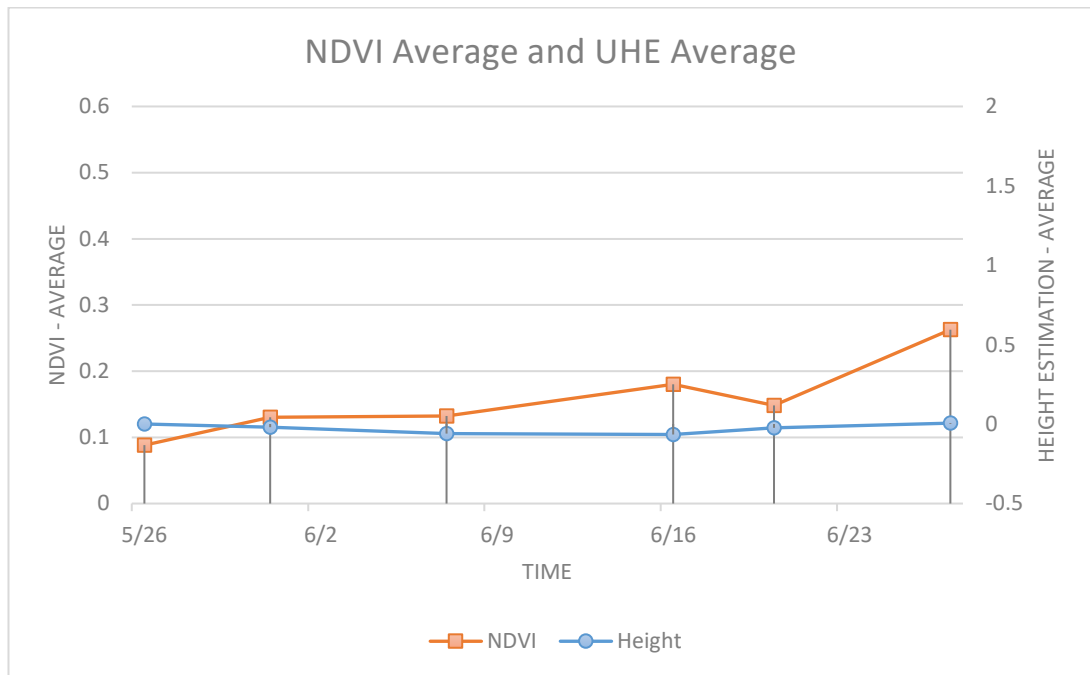


Figure 22: NDVI average and UAV Height Estimation average between May 26th and June 27th

From June 27th until August 17th, UHE field average showed a consistent increase, whilst NDVI field average reaches its saturation on July 22nd (Figure 23).

UHE field average showed a saturation after August 17th, maintaining the same value until September 7th – three weeks later. NDVI field average, presented a small decrease from August 2nd, reaching the 0.406 value on September 7th (Figure 24).

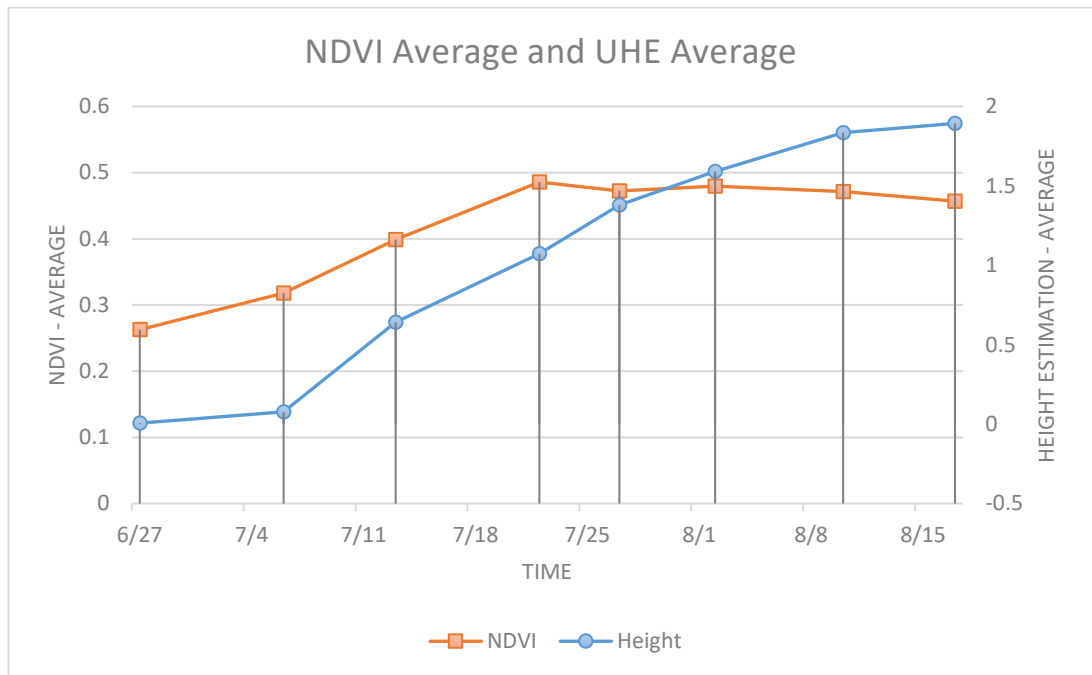


Figure 23: NDVI average and UAV Height Estimation average between June 27th and August 17th

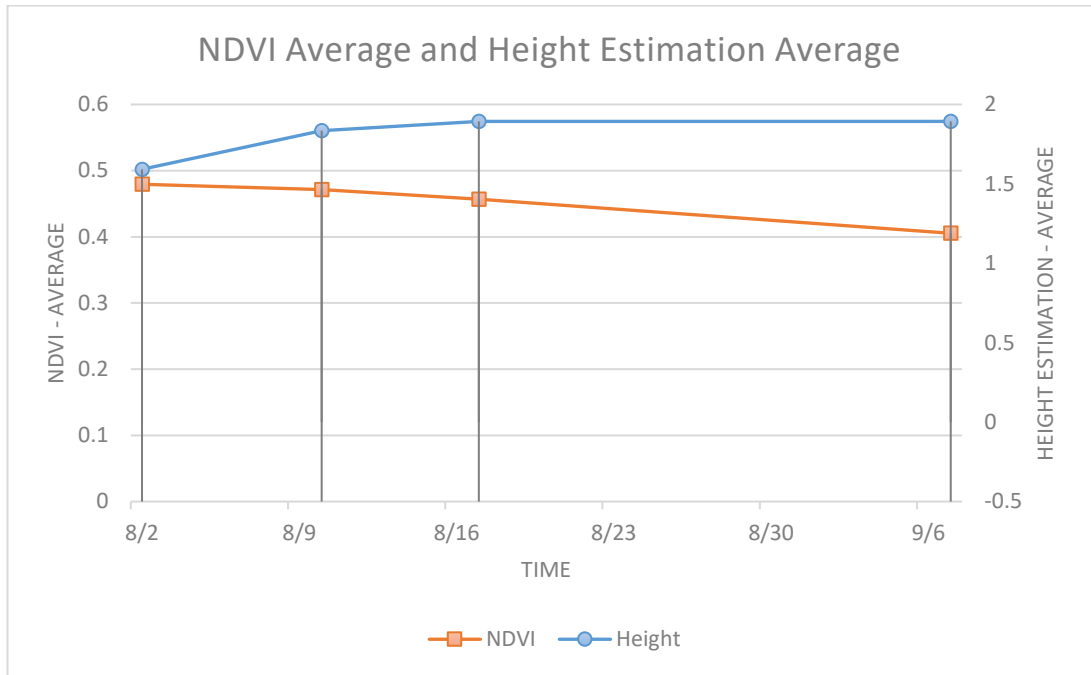


Figure 24: NDVI average and UAV Height Estimation between August 2nd and September 7th

3.4 Field Data

The data measured on the field (Table 2), showed a correlation of 0.43 between Field Measured Height and Dry matter (Figure 25) and a correlation of 0.47 between Field Measured Height and Dry grain yield was 0.47 (Figure 26), considering each grid average.

Code	Ground Measured Height (GMH) (cm)	Dry Matter (g/m ²)	Dry Grain Yield (g/m ²)
E1	247.00	1202.48	527.34
E2	257.00	1270.21	630.46
E3	270.00	1322.64	656.09
E4	265.00	1456.59	680.74
E5	251.00	1418.44	658.36
E6	252.00	1445.53	680.14
E7	238.00	1115.35	468.59
E8	264.00	1484.55	727.44
E9	272.00	1527.42	748.28
E10	272.00	1242.88	599.99
E11	273.00	1477.35	743.18
E12	260.00	1586.01	778.88
E13	236.00	979.08	410.28
E14	263.00	1227.48	595.50
E15	267.00	1364.64	706.65
E16	267.00	1369.74	630.04
E17	260.00	1626.91	796.13
E18	247.00	1393.03	659.01
E19	244.00	1135.32	542.26
E20	259.00	1095.74	472.20
E21	260.00	1388.70	702.17
E22	246.00	1135.26	510.25
E23	249.00	1281.22	630.51
E24	235.00	1182.28	534.21
E25	247.00	1039.27	417.94
E26	264.00	1211.53	581.44
E27	257.00	1135.21	471.92
E28	240.00	1005.37	409.14
E29	256.00	1375.95	697.22
E30	229.00	978.27	399.63
E31	247.00	1056.25	509.55
E32	265.00	1451.59	667.39
E33	245.00	1147.63	552.02
E34	243.00	1117.47	495.68
E35	249.00	1456.77	747.82
E36	233.00	1122.25	470.97

Table 2: Data measured on the field on October 14th

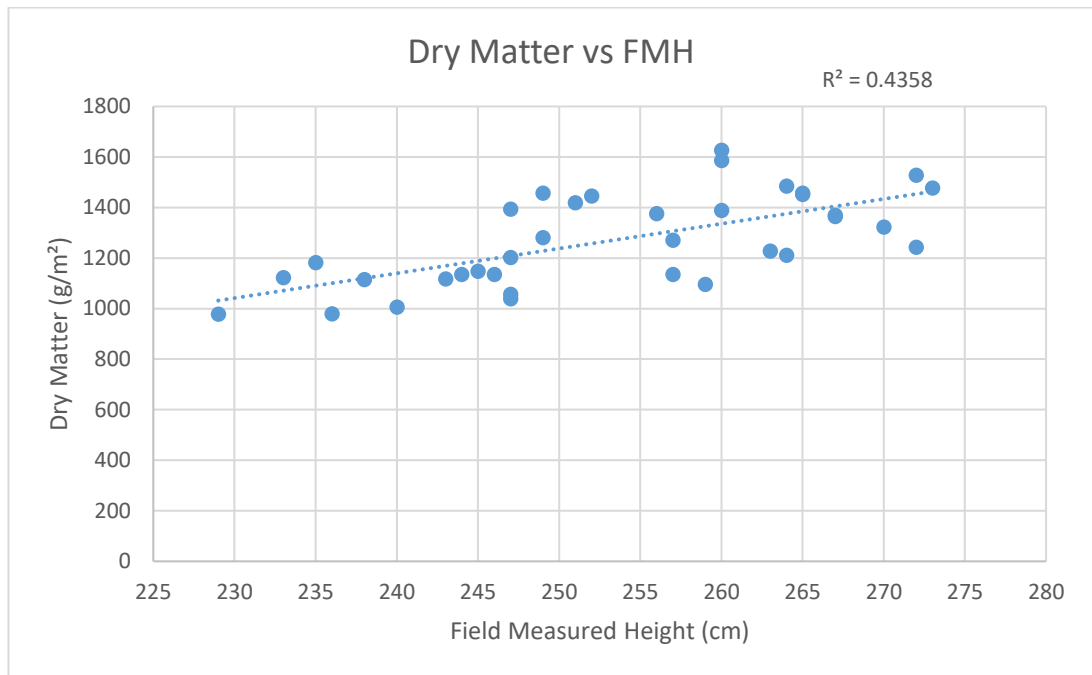


Figure 25: Correlation between Dry Matter measured in the field and Field Measured Height

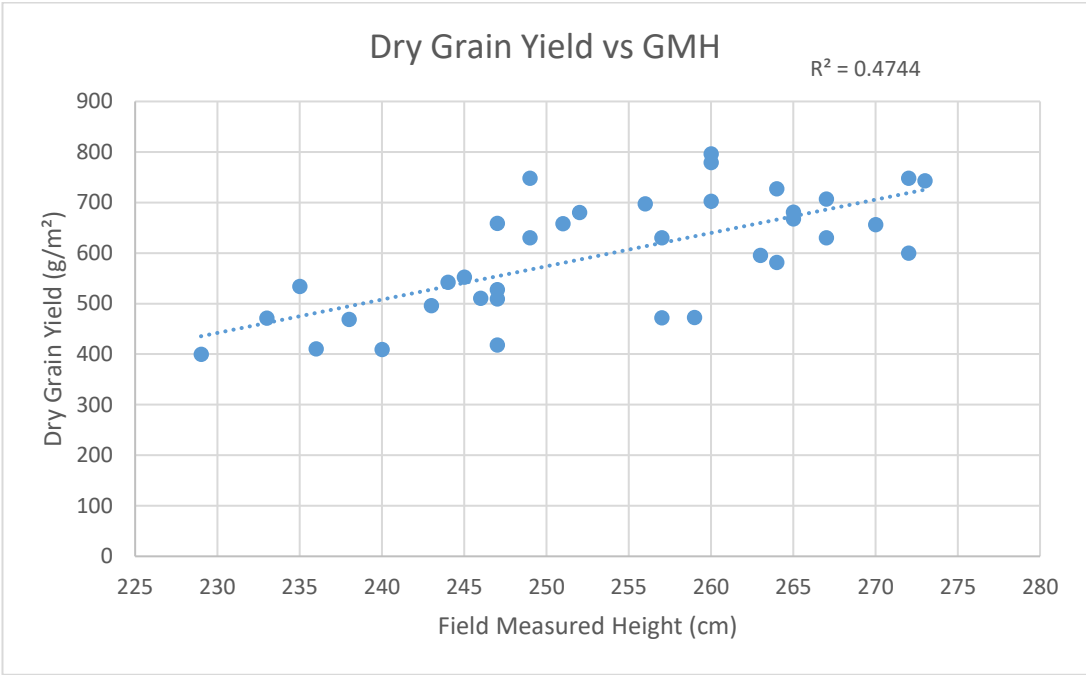


Figure 26: Correlation between Dry Grain Yield and Field Measured Height

3.5 Correlations through Time

The correlation between UAV Height Estimation through time and Dry matter shows R-Squared lower than 0.5 for every date (Figure 27). Comparing UHE with Dry Grain Yield the highest correlation was found on August 2nd with an R-Squared value of 0.510, for the other dates, values lower than 0.5 were find (Figure 28).

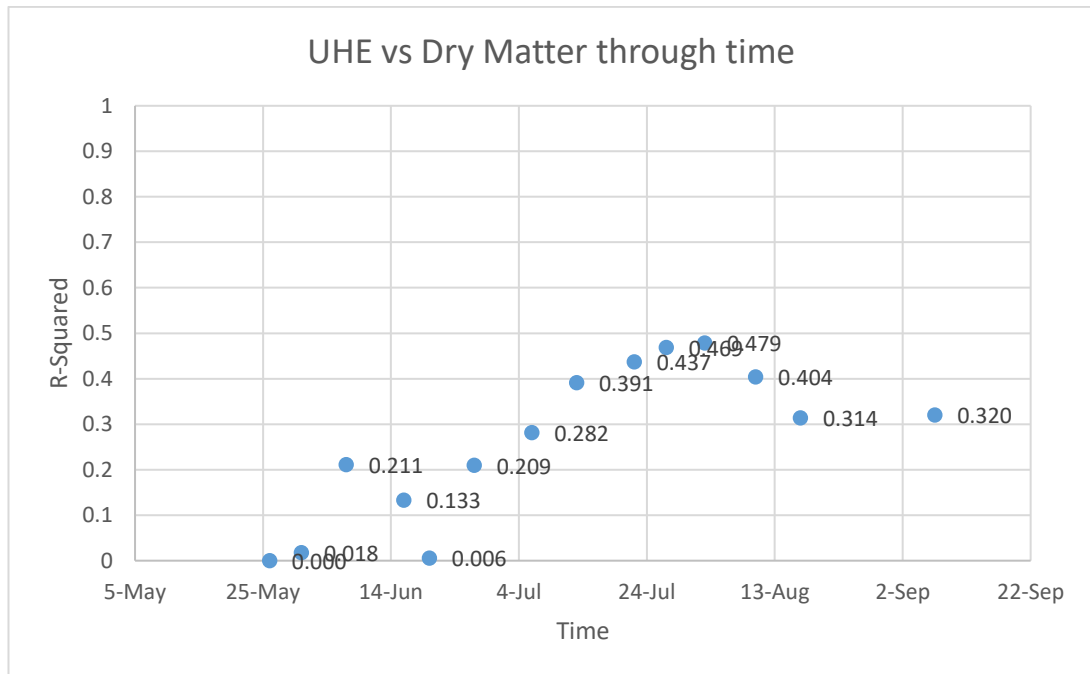


Figure 27: Correlation between UAV Height Estimation and Dry Matter through time

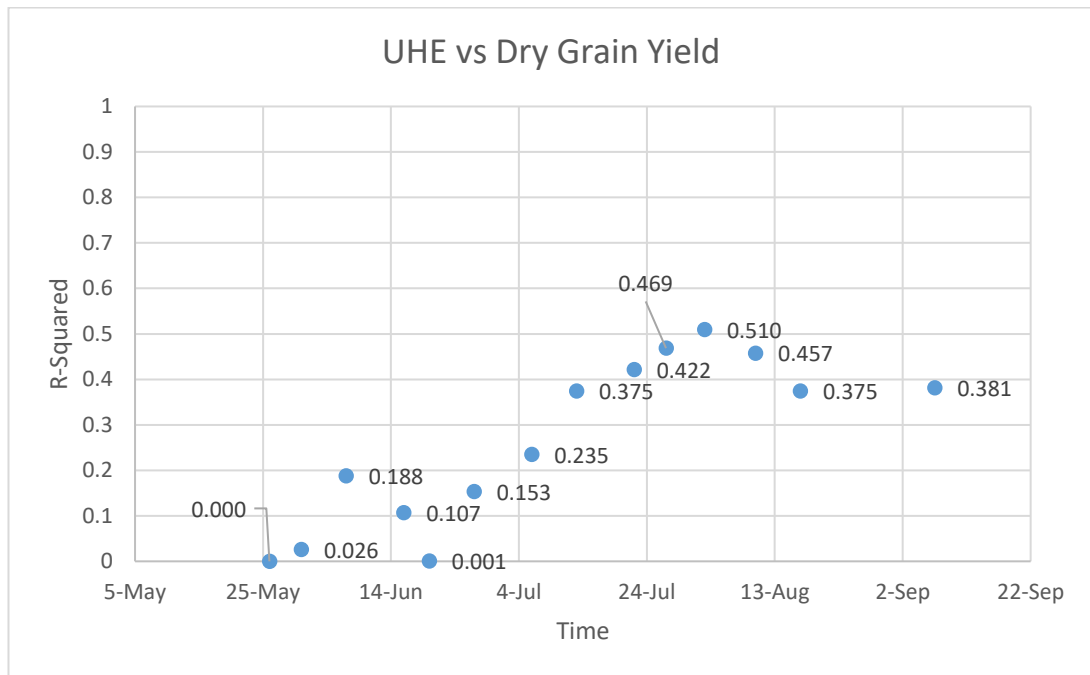


Figure 28: Correlation Between UAV Height Estimation and Dry Grain Yield through time

The same happened with NDVI, with correlation values under 0.5 comparing with Dry Matter (Figure 29) and Dry Grain Yield (Figure 30).

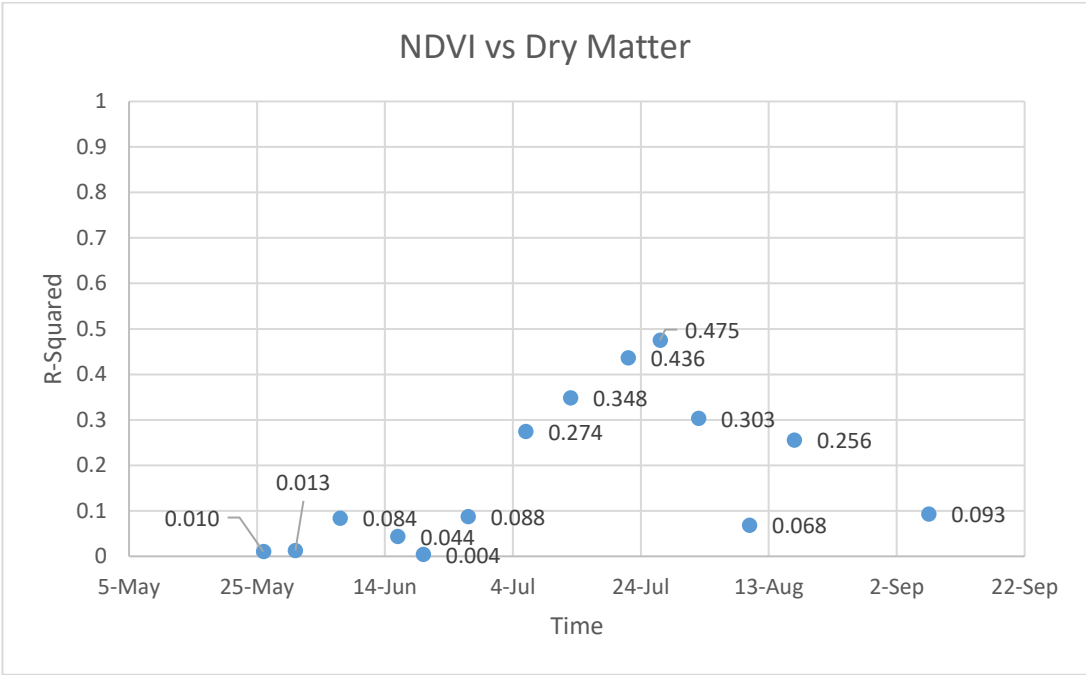


Figure 29: Correlation between NDVI and Dry Matter through time

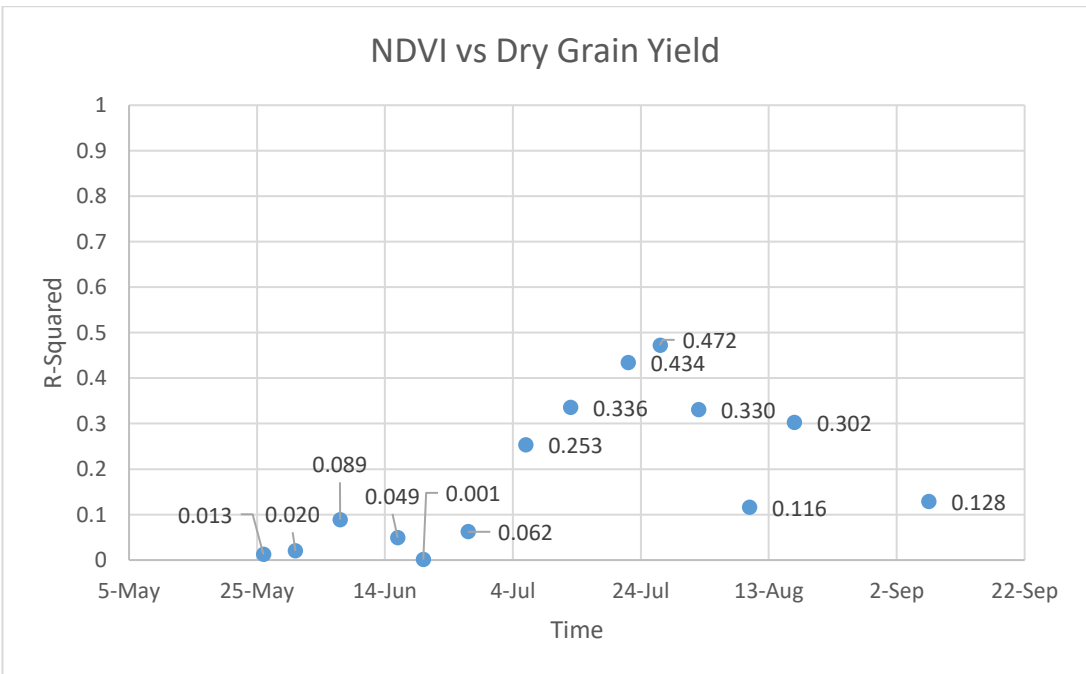


Figure 30: Correlation between NDVI and Dry Grain Yield through time

The correlation between UAV Height Estimation through time and the FMH obtained on October 14th, presented a significant correlation from August 2nd (Figure 31), with an R-Squared of 0.68.

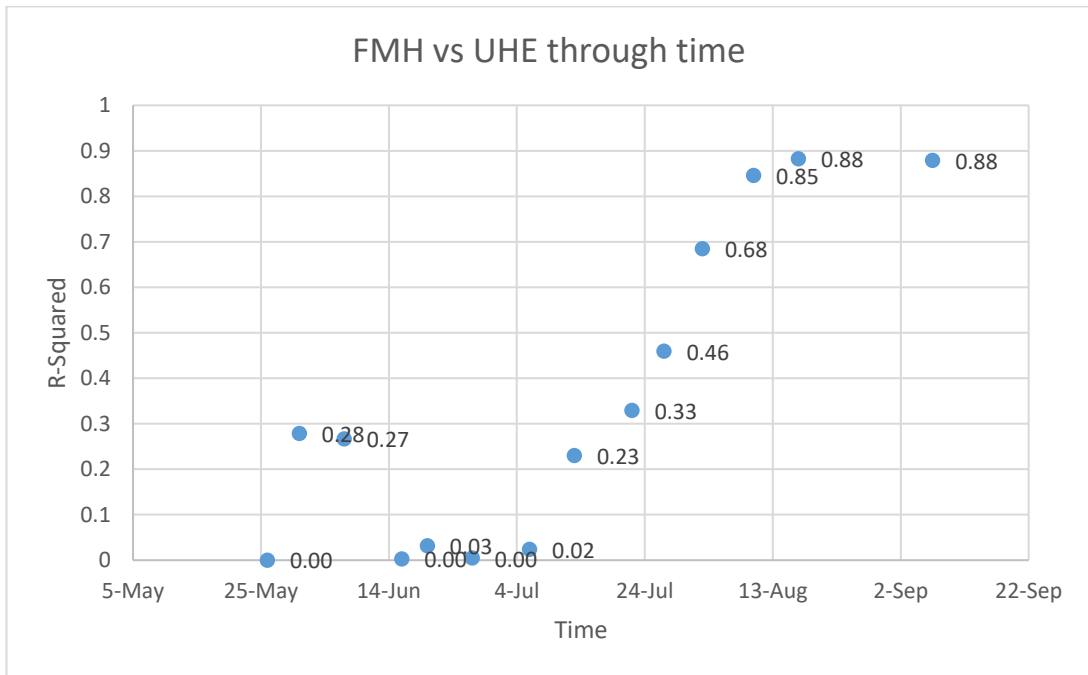


Figure 31: Correlation between Field Measured Height and UAV Height Estimation through time

3.6 Crop Monitoring

Over 14 weeks, the UHE showed the behavior expressed in Figure 32, with a resolution of 2 centimeters per pixel with higher values displayed in magenta and lower values in green.

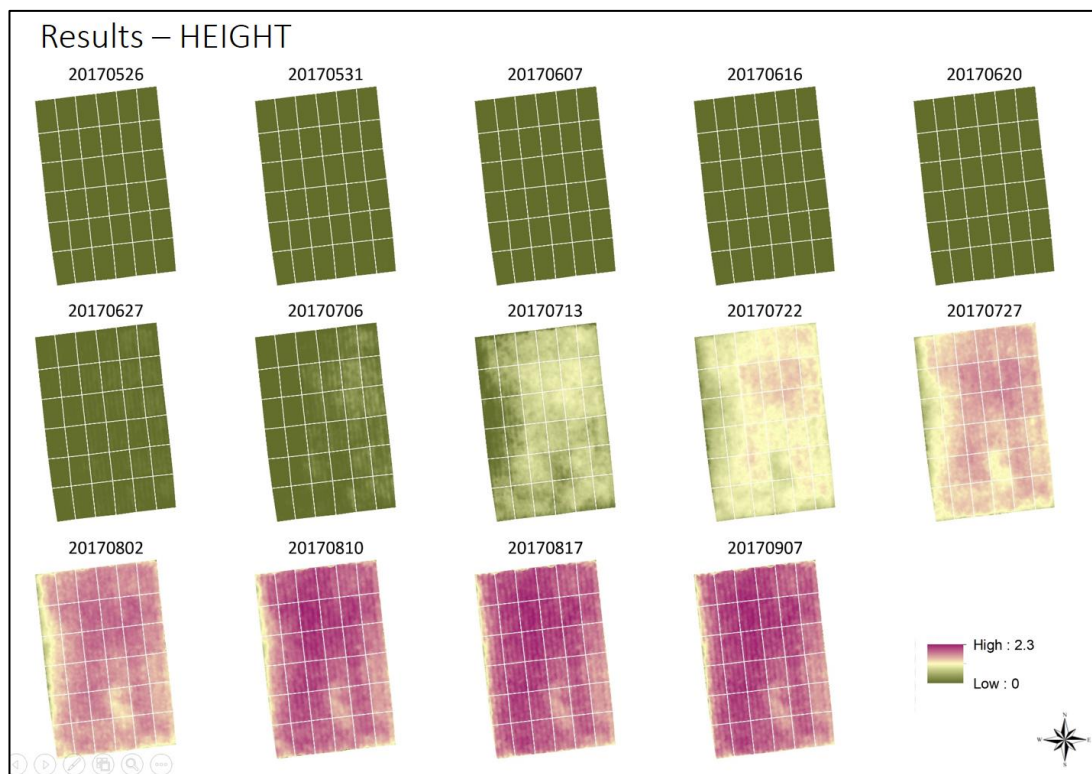


Figure 32: UAV Height Estimation throughout time

NDVI obtained through UAV presented the behavior showed in Figure 33, with 2 centimeters per pixel, with higher values expressed in green and lower values in yellow.

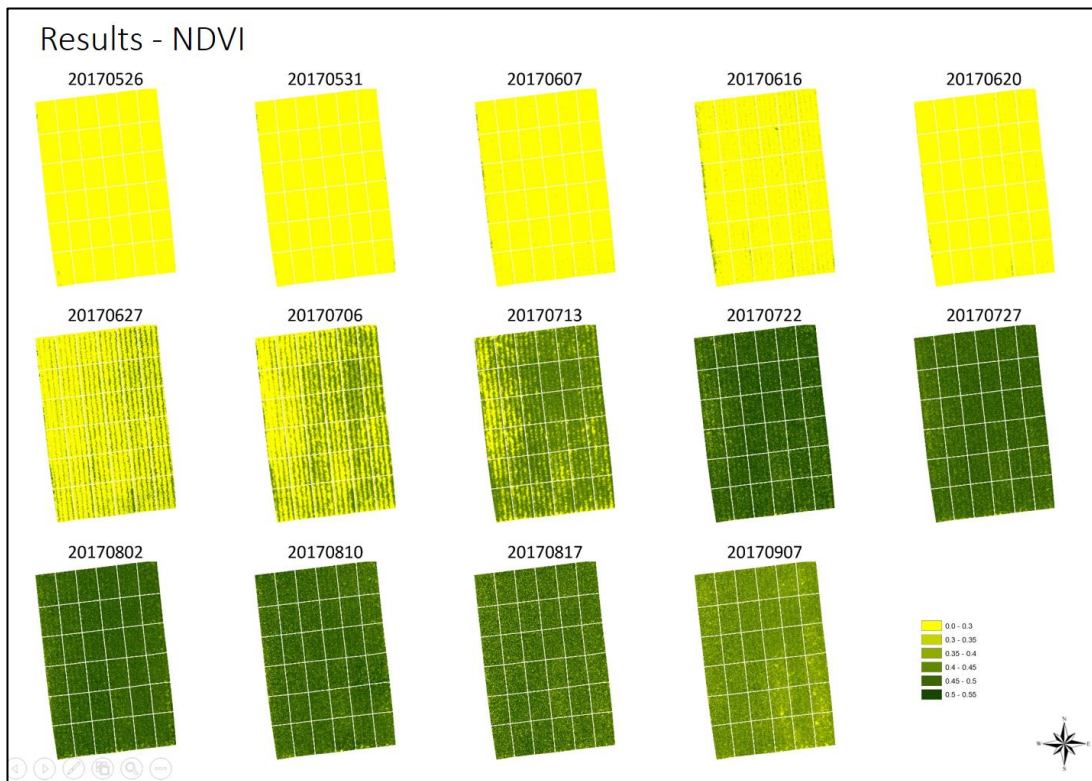


Figure 33: NDVI from UAV throughout time

4. Discussion

The high correlation between satellite data (WV2 and GE1) and UAV data taken with NDVI lens from Peau Productions Inc., presented the capability of the NDVI lens, being possible to estimate NDVI using a low-cost system with high spatial resolution (around 2 centimeters), giving enough details for vegetation analysis.

Since the NDVI average values of each grid were used in this study, a high correlation between NDVI average value obtained with Green Coverage classification and the normal NDVI average was presented (R-Squared of 0.98), the normal NDVI was chosen to be used in this study because of its simplicity, requiring no imagery classification.

NDVI field average obtained through UAV, displayed continuous growth until July 22nd (when reached its saturation), with an exception on June 20th, which the NDVI field average value was lower than the previous data (June 16th). This fact can be explained because of the soil influence on the NDVI average value (Huete, 1988), the same happened with NDVI obtained through Green Coverage classification since the plant is very small, the algorithm classification allowed some soil in the vegetation class. In June 16th and June 27th, the soil moisture was higher than July 20th, changing the color of the soil (Figure 34), causing this lower value.



Figure 34: Different soil moisture among June 16th, 20th, and 27th

Apart from that, NDVI field average data obtained through UAV showed to be very sensitive on early stages of the crop, enabling the ability to follow the growth of the crop. As Strachan et al. (2002) quoted, the plant growth is a function of nitrogen and water availability, understanding the crop growth on early stages, provides more chances to the producer to decide which management is adequate for the situation, improving crop health and enabling the capacity of yield growth monitoring.

On the other hand, UHE field average presented negative values on early stages, until June 20th. This may occur for two reasons: the plants' small size which cannot generate an accurate dense point cloud (Figure 35) and the low accuracy of the cloud alignment through Cloud Compare V.2.8.1 Stereo software. 3D photogrammetry struggles to determine thin or small objects, according to a study by Javernick et al. (2014), the surface vertical error was 10 centimeters, using the same photogrammetry software (Agisoft Photoscan Professional), and also the camera light exposure influences on the final 3D

point cloud (Blizard, 2014). Therefore, the methodology and/or parameters behind point cloud alignment did not present to be suitable for plant growth monitoring at early stages of the crop, some adjustments to the methodology are needed, such as point cloud classification and noise reduction.



Figure 35: Dense point cloud of June 7th

UHE field average had an increasing development from June 27th until August 17th, where reached its saturation. Comparing to NDVI field average, the UHE field average reached its saturation 4 weeks later, allowing plant growth monitoring after the NDVI field average values' saturation and consequently a decrease in its value. Those data showed that even the plant reached the maturity and/or saturation on NDVI, the plants keep growing in height, and even so, UHE enables late stage growth monitoring, when the plants are vulnerable to drought stress, nutrient deficiency or any kind of damage such as hail.

Considering the constant value of UHE from August 17th until September 7th, the significant correlation obtained with October 14th FMH values indicates that the height estimation generated through 3D photogrammetry imagery from UAV, can track plant height growth rate over time through estimation and not real height since 3D Photogrammetry technology presented some limitations to acquiring real size information.

Nevertheless, FMH and UHE start having a significant correlation from August 2nd, enabling crop height prediction 10 weeks before harvest. But in this specific case, the hybrid 36B08 from Pioneer Hi-Bred International, had a small correlation between FMH and Dry Matter, and FMH and Dry Grain Yield, with correlation values lower than 0.5 (0.4358 and 0.4744 respectively), showing that for this specific hybrid, height has no strong relationship with corn yield. Along with that, the correlations between UHE and Dry Matter, UHE and Dry Grain Yield, also had values lower than 0.5, the same happened with NDVI values, consistent with what was achieved with UHE but confronting with Huang et al (2014) where was found a strong correlation between NDVI and crop yield using time series data from MODIS-NDVI.

Although corn yield estimation was not possible in this specific case, UHE showed to be a useful tool for crop monitoring along with NDVI, offering growth data after NDVI saturation, providing a more clear understanding of detecting crop growth comparing to NDVI, due to bigger values difference (Figure 32, Figure 33). Confirming with Bendig et al. (2015) mentioned that the usage of UAV to acquire different indexes and plant height is an exceptional way to acquire data for agriculture purposes, giving a high temporal and spatial resolution with high-cost benefit.

Further studies are necessary to conclude that corn height estimation using a commercial UAV is suitable for corn yield estimation. Manual camera setting and white calibration are recommended to acquire 3D data since light exposure seems to affect in the dense point cloud creation. Along with that, different corn varieties should be tested in order to understand the relationship between corn height and yield.

5. Conclusions

To achieve the food demand by 2050, those agricultural technologies are presenting to be necessary, not only in food production but also to preserve the environment, in other words, sustainable agriculture. Precision agriculture techniques showing its potential to improve agricultural practices in a sustainable way, together with GIS and Remote Sensing technology for crop management and monitoring.

In this research, the main goal was to find the correlation between height estimation using a low-cost Remote Sensing platform with a UAV and corn yield through time, to give enough information in the right time to the producer to take adequate decisions in crop management of all stages, including after harvest.

Even though FMH and UHE could not predict corn yield in this specific case (with the B6B08 hybrid), height estimation using UAVs presented high of potential for yield prediction and crop monitoring, since other researches show the correlation between height and crop yield, such as Yin et al. (2011) presented, it also can be used along with NDVI to assess all stages of the crop, contributing to earlier management decisions.

Further studies with different hybrids are recommended, and improvements on the methodology (in data acquirement and data processing) for height estimation using UAVs are suggested.

6. Acknowledgments

First and foremost, I would like to thank God for His guidance and the strength that He provided me to go through this challenge, for my family, even being in the other side of the planet given me their support, and all my friends which shared this wonderful time that I had in Japan.

I want to thank Mr. Maruyama and the Agricultural department of Rakuno Gakuen University which helped to develop this project, sharing their experiences, knowledge, and data during my research, and the GIS Laboratory staff and students which helped me to process and analyze the data, to discuss and gave me suggestions to improve this project, and not only that, helped me on the small challenges that I had living in a different country with a different culture.

A special thanks to my supervisor, Professor Masami Kaneko for the opportunity provided through these years in Japan, and his guidance, advice and valuable suggestions throughout this challenge, and also JICA, for providing me financial support during this time in Japan and giving the opportunity to experience my ancestors' culture.

7. References

- Bendig, J., Yu, K., Aasen, H., Bolten, A., Bennertz, S., Broscheit, J., Gnyp, M.L., Bareth, G., 2015. Combining UAV-based plant height from crop surface models, visible, and near infrared vegetation indices for biomass monitoring in barley. *Int. J. Appl. Earth Obs. Geoinf.* 39, 79–87. <https://doi.org/10.1016/j.jag.2015.02.012>
- Blizard, B., 2014. The Art of Photogrammetry: How To Take Your Photos - Tested [WWW Document]. Adam Savage's Test. URL <http://www.tested.com/art/makers/460142-art-photogrammetry-how-take-your-photos/> (accessed 1.6.18).
- Bongiovanni, R., Lowenberg-Deboer, J., 2004. Precision Agriculture and Sustainability. *Precis. Agric.* 5, 359–387. <https://doi.org/10.1023/B:PRAG.0000040806.39604.aa>
- FAO, 2009. How to Feed the World in 2050. Insights from an Expert Meet. *FAO 2050*, 1–35. <https://doi.org/10.1111/j.1728-4457.2009.00312.x>
- Haboudane, D., Tremblay, N., Miller, J.R., Vigneault, P., 2008. Remote estimation of crop chlorophyll content using spectral indices derived from hyperspectral data. *IEEE Trans. Geosci. Remote Sens.* 46, 423–436. <https://doi.org/10.1109/TGRS.2007.904836>
- Huang, J., Wang, H., Dai, Q., Han, D., 2014. Analysis of NDVI Data for Crop Identification and Yield Estimation. *IEEE J. Sel. Top. Appl. Earth Obs. Remote Sens.* 7, 4374–4384. <https://doi.org/10.1109/JSTARS.2014.2334332>
- Huete, A.R., 1988. A soil-adjusted vegetation index (SAVI). *Remote Sens. Environ.* 25, 295–309. [https://doi.org/10.1016/0034-4257\(88\)90106-X](https://doi.org/10.1016/0034-4257(88)90106-X)
- Ipate, G., Voicu, G., Dinu, I., 2015. RESEARCH ON THE USE OF DRONES IN PRECISION AGRICULTURE. *U.P.B. Sci. Bull., Ser. D* 77.
- Javernick, L., Brasington, J., Caruso, B., 2014. Modeling the topography of shallow braided rivers using Structure-from-Motion photogrammetry. *Geomorphology* 213, 166–182. <https://doi.org/10.1016/j.geomorph.2014.01.006>
- Matese, A., Toscano, P., Di Gennaro, S.F., Genesio, L., Vaccari, F.P., Primicerio, J., Belli, C., Zaldei, A., Bianconi, R., Gioli, B., 2015. Intercomparison of UAV, aircraft and satellite remote sensing platforms for precision viticulture. *Remote Sens.* 7, 2971–2990. <https://doi.org/10.3390/rs70302971>

- McBratney, A., Whelan, B., Ancev, T., Bouma, J., 2005. Future Directions of Precision Agriculture. *Precis. Agric.* 6, 7–23. <https://doi.org/10.1007/s11119-005-0681-8>
- Ortis, A., Rundo, F., Di Giore, G., Battiato, S., 2013. Adaptive Compression of Stereoscopic Images. Springer, Berlin, Heidelberg, pp. 391–399. https://doi.org/10.1007/978-3-642-41181-6_40
- Pretty, J., 2008. Agricultural sustainability: concepts, principles and evidence. *Philos. Trans. R. Soc. Lond. B. Biol. Sci.* 363, 447–65. <https://doi.org/10.1098/rstb.2007.2163>
- Raun, W.R., Solie, J.B., Johnson, G. V, Stone, M.L., Lukina, E. V, Thomason, W.E., Schepers, J.S., 2001. In-Season Prediction of Potential Grain Yield in Winter Wheat Using Cunopy Reflectance. *Agron. J.* 93, 131–138.
- Rokhmana, C.A., 2015. The Potential of UAV-based Remote Sensing for Supporting Precision Agriculture in Indonesia. *Procedia Environ. Sci.* 24, 245–253. <https://doi.org/10.1016/j.proenv.2015.03.032>
- Rouse, J.W., Hass, R.H., Schell, J.A., Deering, D.W., 1973. Monitoring vegetation systems in the great plains with ERTS. *Third Earth Resour. Technol. Satell. Symp.* 1, 309–317. <https://doi.org/citeulike-article-id:12009708>
- Salamí, E., Barrado, C., Pastor, E., 2014. UAV flight experiments applied to the remote sensing of vegetated areas. *Remote Sens.* 6, 11051–11081. <https://doi.org/10.3390/rs61111051>
- Sawyer, J.E., 2013. Contemporary Issues Concepts of Variable Rate Technology with Considerations for Fertilizer Application 7.
- Spiertz, J.H.J., 2009. Nitrogen, Sustainable Agriculture and Food Security: A Review, in: *Sustainable Agriculture*. Springer Netherlands, Dordrecht, pp. 635–651. https://doi.org/10.1007/978-90-481-2666-8_39
- Strachan, I.B., Pattey, E., Boisvert, J.B., 2002. Impact of nitrogen and environmental conditions on corn as detected by hyperspectral reflectance. *Remote Sens. Environ.* 80, 213–224. [https://doi.org/10.1016/S0034-4257\(01\)00299-1](https://doi.org/10.1016/S0034-4257(01)00299-1)
- Tang, C., Turner, N.C., 1999. *of Experimental Agriculture* 39, 457–464. <https://doi.org/10.1071/EA98132>
- Westoby, M.J., Brasington, J., Glasser, N.F., Hambrey, M.J., Reynolds, J.M., 2012. “Structure-from-Motion” photogrammetry: A low-cost, effective tool for geoscience applications. *Geomorphology* 179, 300–314. <https://doi.org/10.1016/J.GEOMORPH.2012.08.021>

Yin, X., Jaja, N., McClure, M.A., M. Hayes, R., 2011. Comparison of Models in Assessing Relationship of Corn Yield with Plant Height Measured during Early- to Mid-Season. *J. Agric. Sci.* 3, 14. <https://doi.org/10.5539/jas.v3n3p14>